SUPERPLASTICITY IN A DILUTE ZINC ALUMINUM ALLOY

by

RICHARD CHARLES COOK

B.A.Sc., University of British Columbia, 1966

A THESIS SUBMITTED IN PARTIAL FULFILMENT OF

THE REQUIREMENTS FOR THE DEGREE OF

MASTER OF APPLIED SCIENCE

in the Department

of

METALLURGY

We accept this thesis as conforming to the
required standard

THE UNIVERSITY OF BRITISH COLUMBIA

September, 1968

In presenting this thesis in partial fulfilment of the requirements for an advanced degree at the University of British Columbia, I agree that the Library shall make it freely available for reference and Study. I further agree that permission for extensive copying of this thesis for scholarly purposes may be granted by the Head of my Department or by his representatives. It is understood that copying or publication of this thesis for financial gain shall not be allowed without my written permission.

Department of **Metallurgy**

The University of British Columbia
Vancouver 8, Canada

Date Sept 27 /68

ABSTRACT

The system Zn-0.2 wt. % Al has been investigated to determine under what conditions of strain rate, grain size and temperature the phenomenon of superplasticity may be observed.

The analysis and experimental conditions were based on established procedures which have been applied to known superplastic alloys. However the continually decreasing strain rate and grain growth during testing complicate the normal analysis.

Based on this study the requirements for superplastic behavior are a fine-grained microstructure, grain boundaries which are relatively free of obstructions and a homolohous temperature of at least 0.42. A model incorporating grain boundary shear and non-continuous grain growth has been proposed to account for the observed superplastic behavior where grain boundary migration is the rate controlling process.

ABSTRACT

The system Zn-0.2 wt. % Al has been investigated to determine under what conditions of strain rate, grain size and temperature the phenomenon of superplasticity may be observed.

The analysis and experimental conditions were based on established procedures which have been applied to known superplastic alloys. However the continually decreasing strain rate and grain growth during testing complicate the normal analysis.

Based on this study the requirements for superplastic behavior are a fine-grained microstructure, grain boundaries which are relatively free of obstructions and a homolohous temperature of at least 0.42. A model incorporating grain boundary shear and non-continuous grain growth has been proposed to account for the observed superplastic behavior where grain boundary migration is the rate controlling process.

ACKNOWLEDGEMENT

The author is grateful for the advice and encouragement given by his research director, Dr. N. R. Risebrough. Thanks are also extended to fellow graduate students for their many helpful discussions.

Financial assistance was received in the form of an assistantship under National Research Council of Canada grant number A-3675, and is gratefully acknowledged.

TABLE OF CONTENTS

TABLE OF CONTENTS (Cont)

LIST OF FIGURES

LIST OF FIGURES (Cont).

1. INTRODUCTION

The phenomenon of superplasticity has been investigated extensively in the last decade[1-20,27]. Material from numerous metal systems including those of eutectic, eutectoid and essentially phase pure composition exhibit the ability to withstand large amounts of neck-free deformation. Interest has been focussed on the search for a deformation mechanism which is consistent with the tensile and metallographic observations. On the other hand, the implications of the possible advantages in a metal-forming operation have not been overlooked[3,5].

The basis for superplasticity is a strong dependence of the flow stress (σ) on the imposed strain rate ($\dot{\varepsilon}$). These parameters are usually related through the relationship[3]:

$$\sigma = K\dot{\varepsilon}^m$$

where K is a constant and m is the strain rate sensitivity parameter. Values of m vary from less than 0.1 for most metals up to 1.0 for hot polymers and glasses. At strain rates where m is high, the region of an incipient neck will be hardened due to the localized increase in strain rate and the deformation proceeds in the softer regions of the sample. Thus it is apparent that for a sufficiently high value of m (approximately 0.3 to 0.7), large amounts of deformation (up to 2000% elongation)[23] can be obtained. It is known that superplasticity can be obtained in a system where a structural phase change occurs during deformation. Thus earlier studies were concerned with two phase alloy systems and it was thought that the requirements[2] were a diffusion-controlled structural change concurrent with the deformation and a homologous temperature greater than 0.5. More recent investigation has shown that a phase change is not a necessary requirement and the most important structural condition is a finely divided microstructure[4-12]. This requirement is easily

satisfied in two phase systems since a stable, fine-grained microstructure is readily obtainable.

The most extensively studied systems have been the eutectoid Zn-22 wt. % Al and the Sn-Pb alloy systems. The eutectic/eutectoid alloy systems generally all require a hot working step to produce large numbers of intercrystalline boundaries before the material behaves superplastically and they possess the characteristic of having two phases which constitute about equal volume fractions of the alloy. As opposed to this type of system, extensive work has been carried out on essentially phase pure systems: Gifkins[22] on Pb-2-8% Th., Cline and Alden[7] on Sn-2wt. % Pb, and pure Sn, Alden on Sn-5wt. % Bi[6], Sn-1wt. % Bi[19], and Floreen[27] on pure Ni. Since it has been generally accepted that a fine-grained microstructure, along with a homologous temperature greater than 0.5, is essential to the superplastic phenomenon, the inherent problem in all these systems has been to achieve and retain a fine grain size in the test material. Thus, the role of the small additions of a second-phase material has been similar to the role played by interphase boundaries in two phase materials, that is, to restrict grain growth during material and specimen preparation.

Several possible mechanisms have been proposed to account for the high rate sensitivities and the large amounts of elongation that have been observed in these systems.

a) Holt[12] suggested a model for the Zn-Al eutectoid system which was based on grain boundary shear and associated migration of the boundaries to relieve stress concentrations at triple points. This suggestion is further supported by Holt and Backofen[8] in the Al-33 wt. % Cu eutectic system where it was proposed that grain boundary shear was the rate controlling process and that mechanical obstructions to sliding were

removed through strain rate enhanced boundary migration or recrystallization. Grain boundary sliding was also proposed by Alden[6-7] to be the rate controlling process in Sn-Bi and Sn-Pb alloys and it was shown[7] that the contribution of boundary shear to deformation was greatest at the maximum value of the rate sensitivity parameter m. At high strain rates where m values are low, it was found that deformation became slip controlled and superplasticity was not observed.

b) The eutectic system Sn-38 wt. % Pb was examined by Avery and Backofen[4] and they proposed that two competitive processes contributed to the deformation. One involves dislocation motion which accounts for the low rate sensitivity at high strain rates and the other is viscous flow associated with Nabarro-Herring (N-H) diffusional creep. The Coble variant of the N-H analysis was suggested by Jones and Johnson[26] in a discussion of Backofen's work on the Sn-Pb system[4]. This model is based on grain boundary diffusion rather than volume diffusion and it was suggested that it predicted the deformation behavior more accurately than the normal N-H analysis.

c) Zehr and Backofen[11] suggested that grain boundary shear acting in parallel with diffusional creep accounts for the high rate sensitivity and metallographic observations observed at low strain rates in the Sn-Pb system. Experimental flow stress-strain rate relationships could be reproduced by semi-empirical procedures based on this model.

d) Packer and Sherby[17] proposed a modification to Avery and Backofen's[4] analysis of the data for the Sn-Pb eutectic system. They have suggested that a model based on recrystallization or grain boundary migration associated with a dislocation-climb-controlled process results in better agreement with high rate sensitivity and microstructural effects observed. Further to this suggestion Hayden et al[14] have proposed that the mechanism

of superplastic flow may be similar to the recovery creep mechanism of Mott[28] and Friedel[29] based on dislocation climb. Their results on the two-phase Ni-Fe-Cr system do not support a model based on N-H diffusional creep. In support of this argument Kossowsky and Bechtold[18] have examined the Zn-Al eutectoid system and have proposed that a dislocation climb mechanism is rate controlling and predicts the correct values for the rate sensitivity observed.

e) Alden, in a recent proposal[20], has postulated a climb-glide dislocation process which would support a model based on grain boundary sliding. It is suggested that the glide component contributes directly to sliding but that it is the climb component which is rate determining.

Most of the above interpretations have been based on an analysis of m values and correlations between flow stress and grain size. Metallographic observations have generally been restricted to the structures present after relatively small amounts of deformation (<50% strain).

In the present work an alloy of Zn-0.2 wt. % Al has been prepared by casting and final extrusion to achieve a fine-grained, equiaxed microstructure. This system was chosen so the tensile behavior of the Zn-rich solid solution of the eutectoid alloy could be studied. It should be noted that previous studies on the eutectoid have been carried out at high homologous temperatures (T_H = 0.9 based on the invariant temperature). The tensile behavior has been investigated over a range of temperatures to determine the conditions under which superplasticity might be obtained.

2. EXPERIMENTAL

2.1. Material Preparation

A master alloy of 5.5 wt. % Al was prepared using special high purity zinc (99.999%) and aluminum (99.995%). Materials were prepared

either by a casting or shotting procedure following the dilution to the desired alloy composition of Zn-0.2 wt. % Al. Melting was carried out at temperatures of 700-750°C under a flux cover of NaCl-50% KCl to prevent excessive oxidation of the zinc. The melt was held at 700°C for 30 minutes prior to casting or shotting to insure complete dissolution of the aluminum in the zinc.

2.1.1. Extruded Castings

The melt was chill cast from 700°C to give billets of approximate dimensions 2.5 in. by 0.9 in. diameter. The billets were homogenized at 350°C for 60 hours in order to redissolve all the Al-rich second phase and were then water quenched, to produce a fine, randomly distributed precipitate. After reducing the diameter of the billet to approximately 0.75 in. two different extrusion procedures were used. In order to achieve a fine grain structure the temperature of extrusion must be kept as low as possible and to this end a billet was wrapped in lead foil and hot extruded in a single operation at 80°C with a pressure of 144,000 psi (extrusion ratio 42:1) the grain size obtained was 3.5 microns. To achieve a finer grain size, a second billet was extruded at 30°C and a pressure of 144,000 psi utilizing Carbowax 1500 as a die lubricant. Using this procedure the grain size was reduced to 1.6 microns (Fig. 1a). The extruded rods of 0.15 in. diameter were stored in liquid nitrogen within 15 minutes of extrusion.

To determine the effect of the solute addition, pure zinc (99.999%) was chill cast, homogenized under similar conditions and hot extruded at room temperature and 144,000 psi pressure using Carbowax 1500 as a lubricant. Again, the extruded rods were immediately stored in liquid nitrogen.

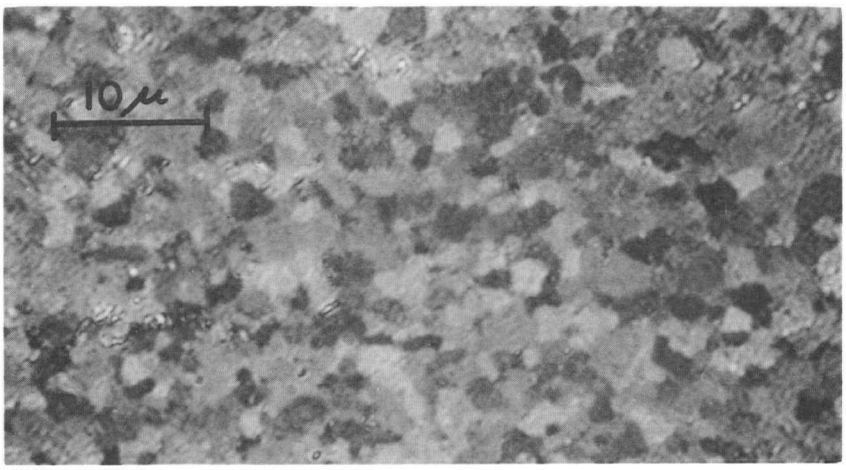

a) Cast and extruded material. L = 1.6 microns.

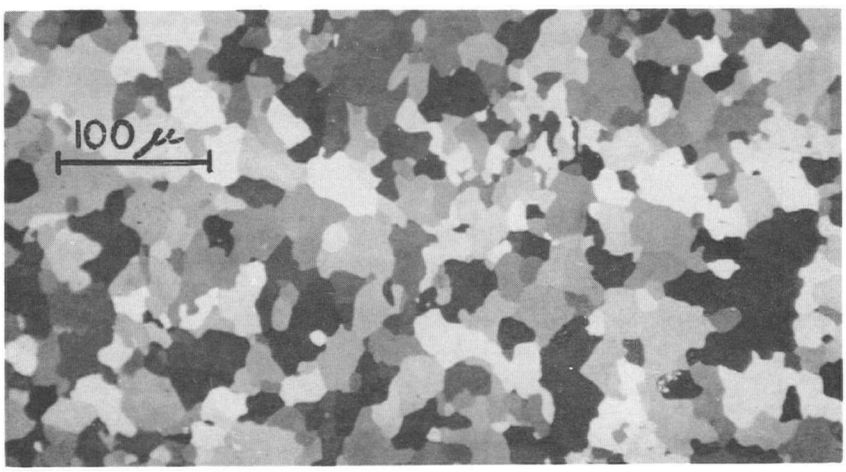

b) Cast and rolled material, L = 16 microns.

Fig. 1. Microstructure of Zn - 0.2 wt. % Al.

2.1.2. Extruded Powders

The melt of identical composition was held at 700°C for 30 minutes and then was subjected to a powder making procedure as developed by Waldron et al*. Powders in the size range -200 mesh were compacted hydrostatically into billets approximately 3 in. by 0.75 in. diameter. The billets were hot extruded to a final diameter of 0.150 in. utilizing 104,000 psi extrusion pressure and a temperature of 270°C.

2.1.3. Rolled Material

The melt was cast into 0.5 in. x 1.5 in. x 5 in. billets which were subsequently homogenized in air at 350°C for 25 days and water quenched. The billets were cropped and machined to remove surface irregularities prior to hot rolling. To avoid cracking due to the initially large grain size, rolling was carried out at approximately 300°C and reduced the thickness of the billet to 0.125 in. Grain refinement was achieved by rolling at room temperature in steps of 0.010 in. to a final thickness of 0.045 in. Following this procedure a completely recrystallized, equiaxed microstructure was obtained (Fig. 1b).

2.2. Specimen Preparation

For the extruded material, tensile specimens were machined on a jeweler's lathe to a reduced diameter of 0.075 in. $\pm$ 0.0005 in. over a gauge length of 0.65 in. $\pm$ .01 in. Specimens prepared from extruded castings did not exhibit the grain size stability of those extruded from compacted powders and hence the heat generated during the machining was apparently sufficient to cause a slight increase in grain size. For

---

* Procedure given in private communication with R. J. Waldron.

this reason, a cold machining technique was devised whereby dry nitrogen at a temperature of approximately -50°C was used to cool the specimen in the lathe. Using this technique on all samples prepared from extruded castings it was possible to minimize the apparent problem of grain growth prior to testing.

For the rolled material tensile specimens of 0.65 in. gauge length and 0.200 in. x 0.045 in. cross-section were spark-machined from the strip. Damage due to spark machining was negligible.

2.3. Tensile Procedures

All tensile tests were conducted on a Floor Model Instron utilizing constant cross-head speeds which varied from 2×10^{-4} in./min. to 2 in./min. Testing media included cooled ethyl alcohol (-100°C to 0°C), heated water (22°C to 100°C), and silicone oil (above 100°C). Temperature control was $\pm$ 2°C in all cases.

For the rolled specimens gripping was achieved by a split jaw grip arrangement and for the extruded specimens by a split, button head grip which gripped only on the shoulder region. Tensile tests were of two different types. The first was a normal tensile test in which the specimen was strained to failure at a constant crosshead speed. The second, in which the crosshead speed was changed incrementally from 2×10^{-4} in./min. to 2 in./min., allowed an evaluation of the strain rate sensitivity parameter as described by Avery and Backofen[3] (see also Appendix I). At any strain rate, when it appeared that a steady state stress had been reached, the strain rate was increased by a factor of 2 or 2.5. The amount of strain at each strain rate was usually of the order of 3 to 4% so that the total amount of strain per test was approximately 30 to 40%.

The values for true stress and true strain rate have been calculated on the basis of instantaneous area and length which were calculated assuming uniform deformation throughout the entire gauge length of the specimen.

2.4. Metallography

Electropolishing was found to be the most convenient and reliable method of preparing a surface for metallographic observation. Polishing time was approximately 30 seconds at a current density of 0.8 amp/cm^2 which corresponded to the plateau voltage. The polishing solution was as follows:

800 ml	Ethyl Alcohol
50 ml	Butylcellusolve
60 gm	Sodium thiocyanate
20 ml	Distilled water

Most observations were carried out using polarized light to reveal the zinc grain structure. The second phase aluminum - rich particles were apparently randomly distributed throughout the zinc matrix. A separate metallographic study was made on two-stage chromium shadowed replicas taken from a prepolished deformed specimen. Fine scratches imposed on the specimen surface prior to deformation facilitated observations on grain boundary shear and grain rotation.

Grain size was determined by the line intercept method using at least two random photomicrographs which exhibited approximately one hundred intercepts on a series of lines drawn both perpendicular and parallel to the tensile axis. Microstructural control was achieved by annealing the samples at elevated temperatures for periods of time sufficient to obtain the desired grain size. The various thermal and mechanical treatments used to obtain the initial grain sizes are summarized in Table I.

TABLE I

MECHANICAL AND THERMAL TREATMENT APPLIED TO Zn- .2 wt. % Al

Alloy Designation	Description	Thermal Treatment	Grain Size (Microns)
A	Extruded casting @ 30°C	as extruded	1.6
	"	15 min. @ 100°C	3.5
B	Extruded casting @ 80°C	as extruded	3.5
	"	15 min. @ 100°C	3.7
		24 min. @ 150°C	4.7
		30 min. @ 200°C	7.2
C	Rolled Casting	as rolled	16
	"	15 min. @ 150°C	23
	"	25 min. @ 150°C	27
	"	30 min. @ 250°C	66
D	Extruded powders @ 270°C	as extruded	2

3. RESULTS

3.1. Extruded Castings

3.1.1. Preliminary Investigation

As described in the previous section, the materials used for the present investigation were of similar composition but the resulting structure varied due to the different methods of preparing the final tensile specimen. Data obtained from the tensile behavior of specimens machined from the extruded cast billets will be presented first followed by data from the extruded powder compacts and the rolled stock.

3.1.2. Grain Size Effect

A typical stress-strain rate relationship for superplastic materials is shown in Fig. 2. Alden[6] has proposed that the low rate sensitivity at high strain rates is due to slip controlled deformation while the regions of high rate sensitivity can be shown to be associated with grain boundary sliding.

The flow stress-strain rate relationships found in Zn-0.2 wt. % Al at +23°C exhibit the characteristic S-shaped curve (Fig. 3). At intermediate strain rates a region of high rate sensitivity exists and is bounded at high and low strain rates by regions of low rate sensitivity. The flow stress at low strain rates is drastically affected by the preparation history of the material. Curve B illustrates the high rate sensitivity observed when cold machining is utilized in specimen preparation as opposed to Curve C which is typical for a hot machined specimen. By decreasing the temperature of extrusion and thus decreasing the grain size in the extruded rod the behavior is again affected as shown by Curve A. For comparison, Curve D is included to illustrate the low rate sensitivity at all strain rates in the material extruded from a powder compact. The reasons for this behavior will be discussed in a later section.

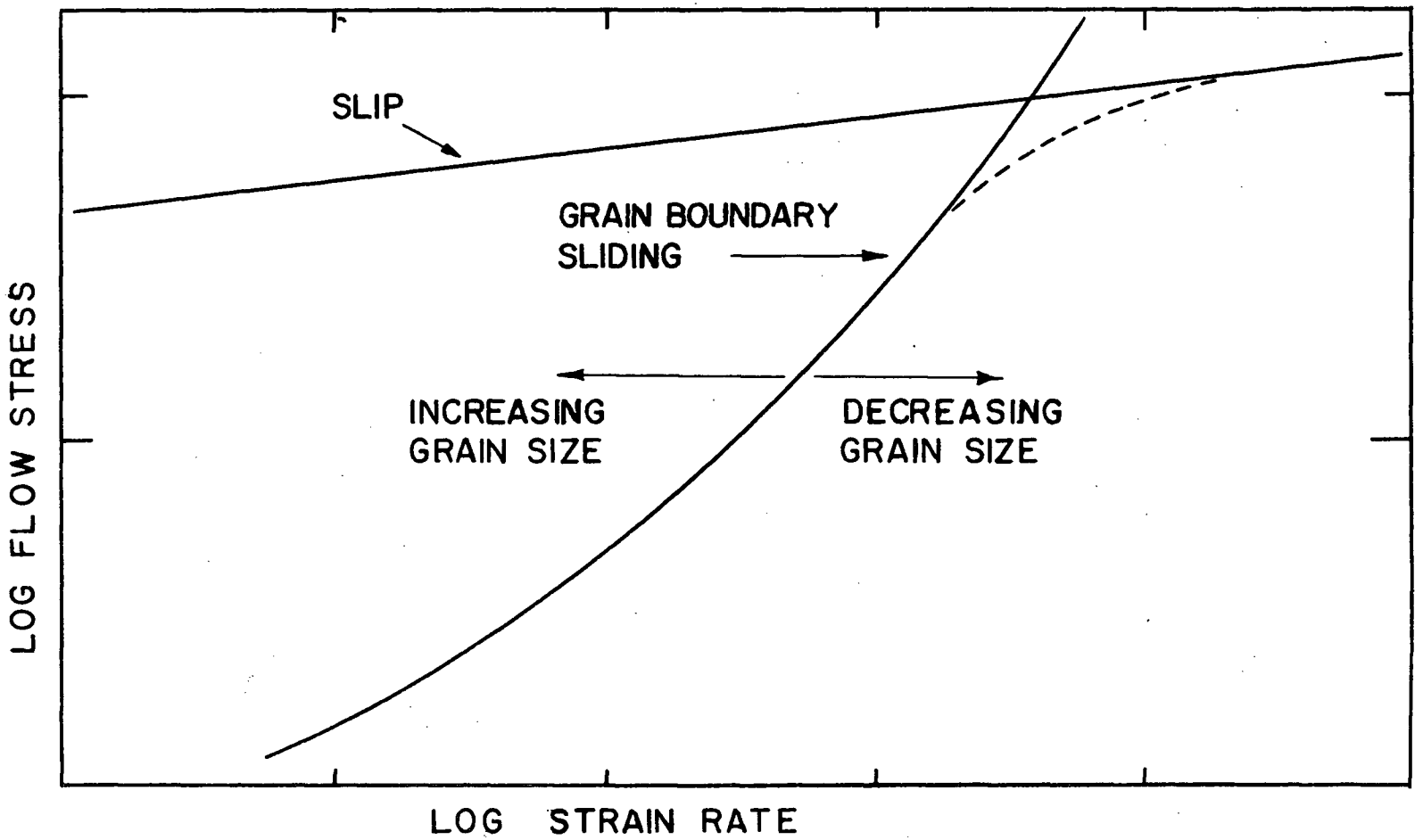

Fig. 2. Origin of S-shaped log σ - log $\dot{\varepsilon}$ curve (schematic). The dominant deformation mode at low strain rates is grain boundary sliding, at high rates slip. (after Alden[6]).

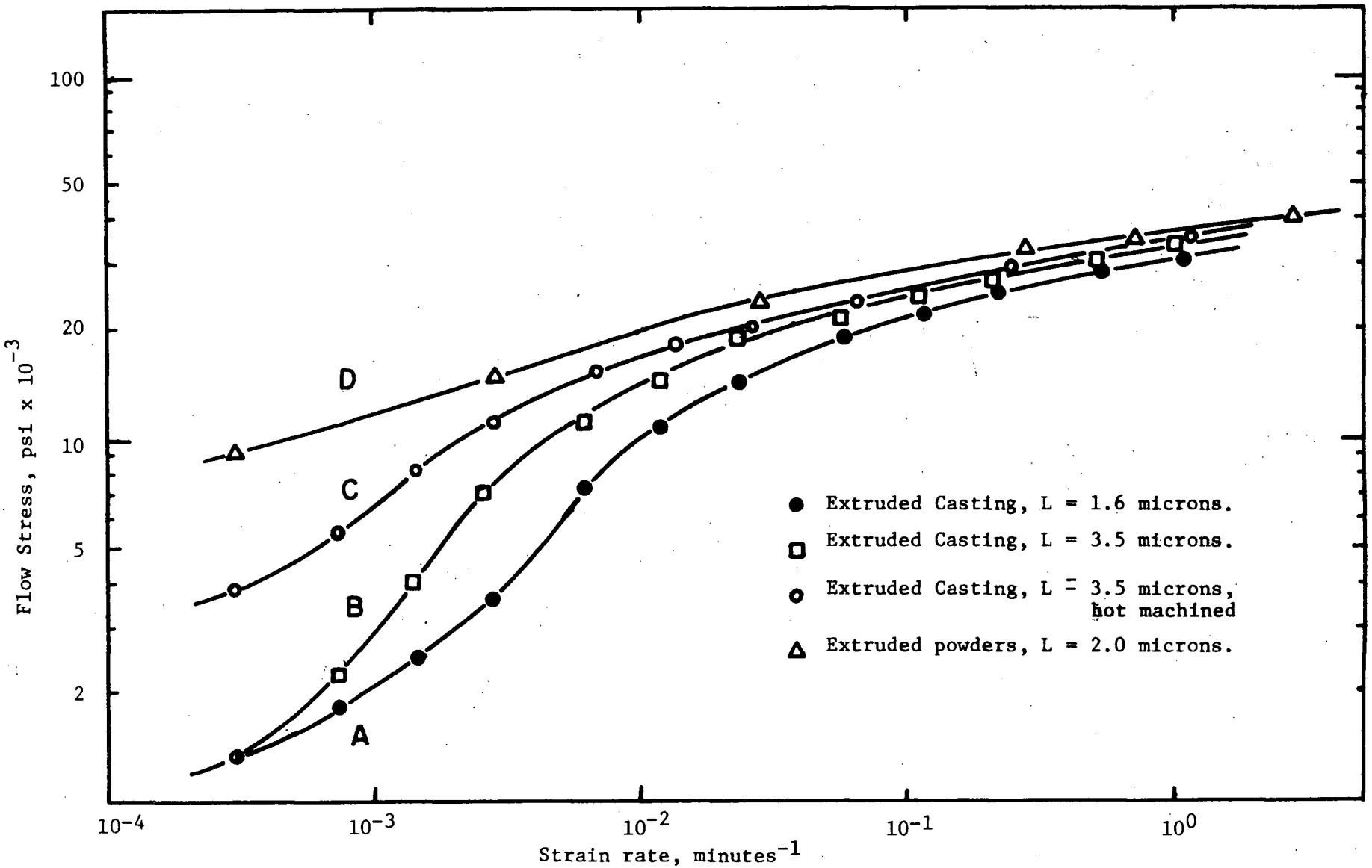

Fig. 3. The effect of preparation history on the stress-strain rate relationship for extruded material. T = + 23°C.

For a more detailed examination of the relationship between flow stress and grain size, thermal treatments were used to obtain a variety of grain sizes (Table I). The flow stress-strain rate relationships are shown in Fig. 4. The effect of decreasing the grain size is to shift the curves down and to the right, that is, to shift the region of maximum strain rate sensitivity to a higher strain rate. At high strain rates (greater than 1 min^{-1}) the flow stress appears to approach a value independent of grain size while at low strain rates the flow stress is significantly lower for the finest grained material. These observations are consistent with those made on known superplastic materials.[6]

Values of the strain rate sensitivity parameter m may be obtained from a direct measurement of the slope of the curve relating flow stress to strain rate on logarithmic co-ordinates ($m = \partial \ln \sigma / \partial \ln \dot{\varepsilon}$). Alternatively, m can be calculated from the flow stress increment accompanying an isolated strain rate change by a technique described by Avery and Backofen[3] (see Appendix I). The latter method has been used in this work and the values of m as a function of strain rate for the different grain sizes are shown in Fig. 5. and Fig. 6. The effect of decreasing the grain size is to shift the region of maximum m to higher strain rates due to the increasing contribution of boundary shear. One should note that the only difference between the data in Fig. 5 and 6 is the as extruded grain size.

The data of Fig. 5 from the material with the smallest grain sizes illustrate that the rate sensitivity rises to a maximum value as strain rate is increased. For the larger grained material this peak value was not observed due to the mechanical limitations of the testing procedure. At higher values of strain rate, the rate sensitivity is

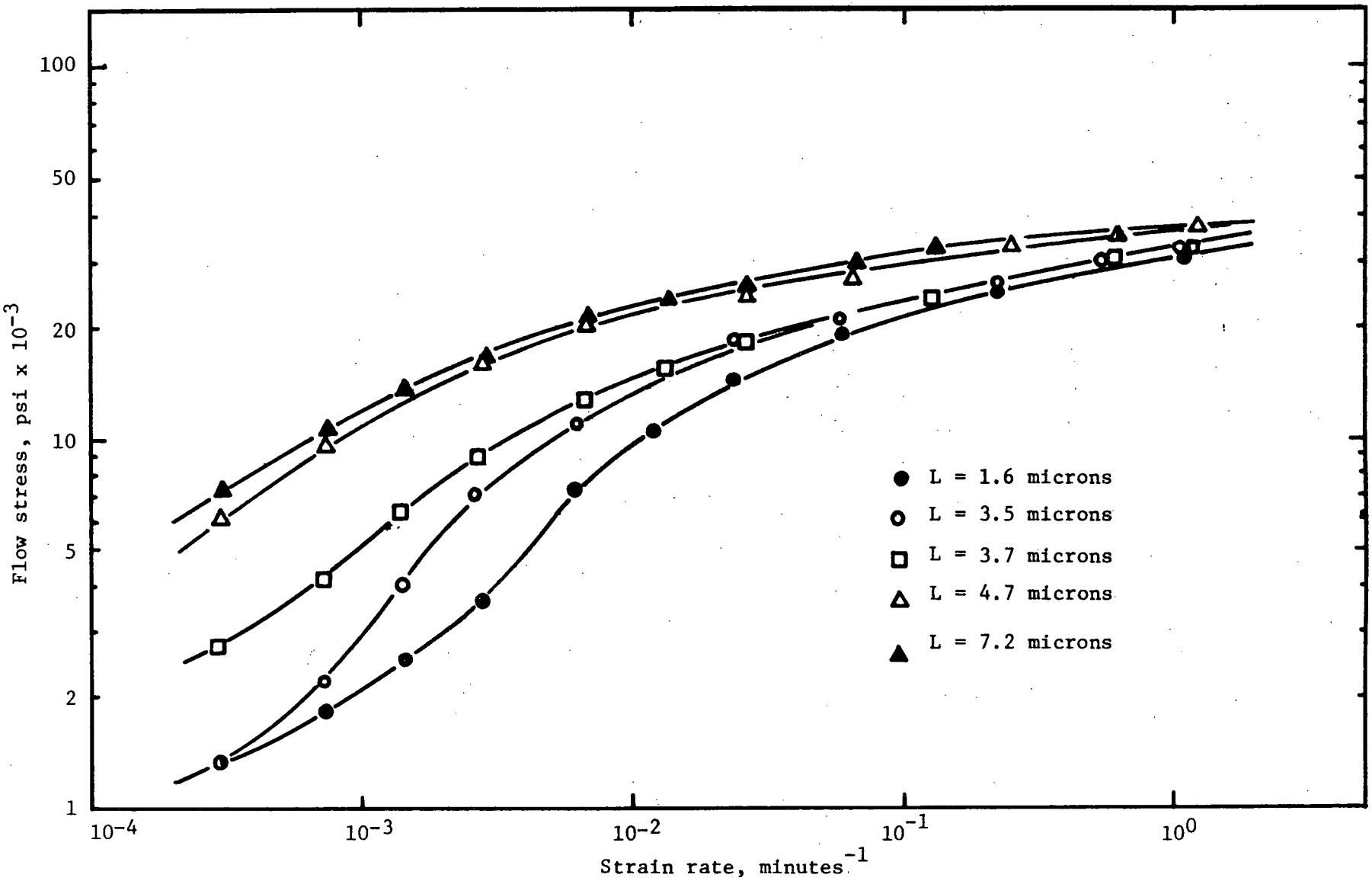

Fig. 4. The effect of grain size on the stress-strain rate relationship for extruded material. T = +23°C.

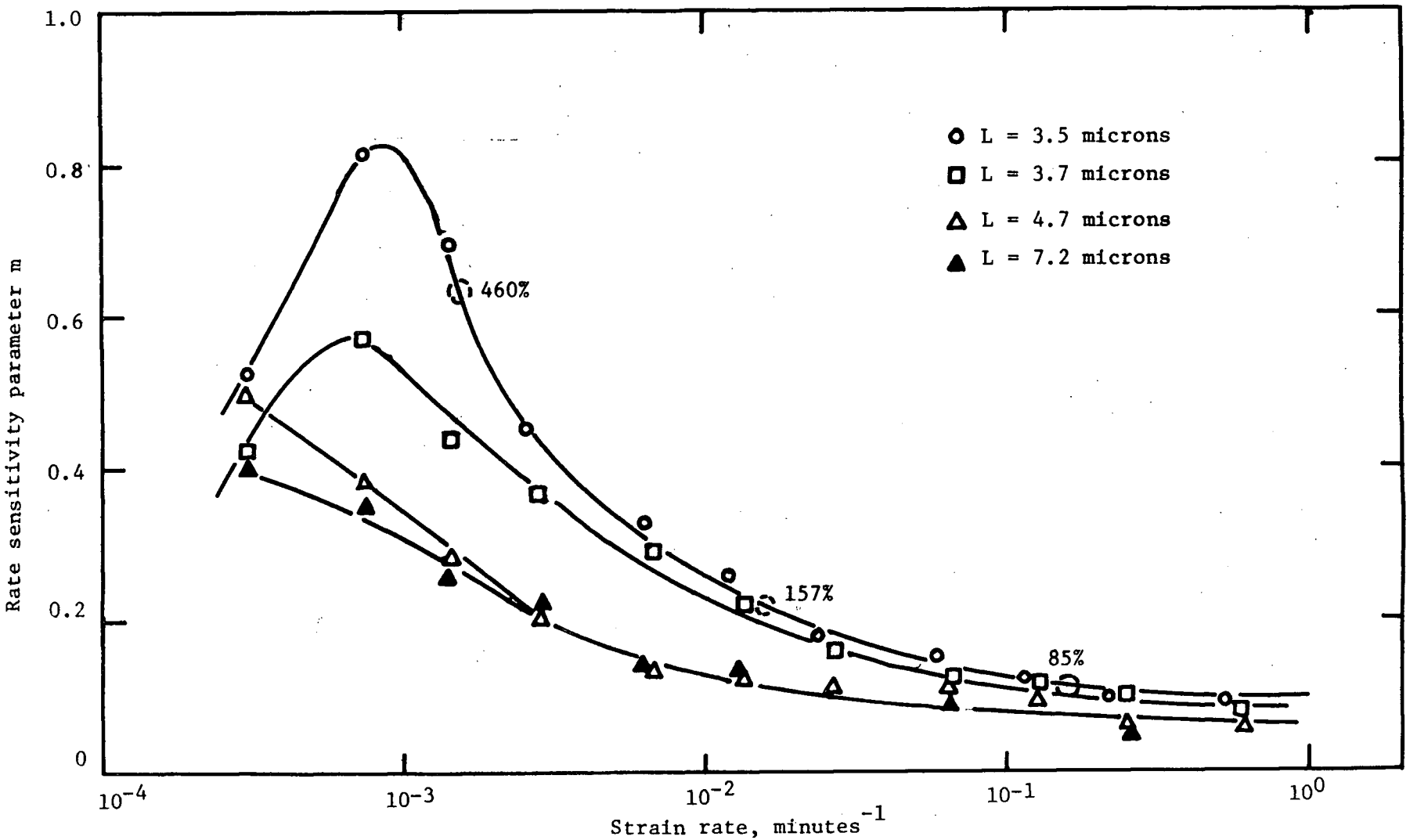

Fig. 5. The relationship between the rate sensitivity parameter m and strain rate. T = +23°C L = 3.5 microns.

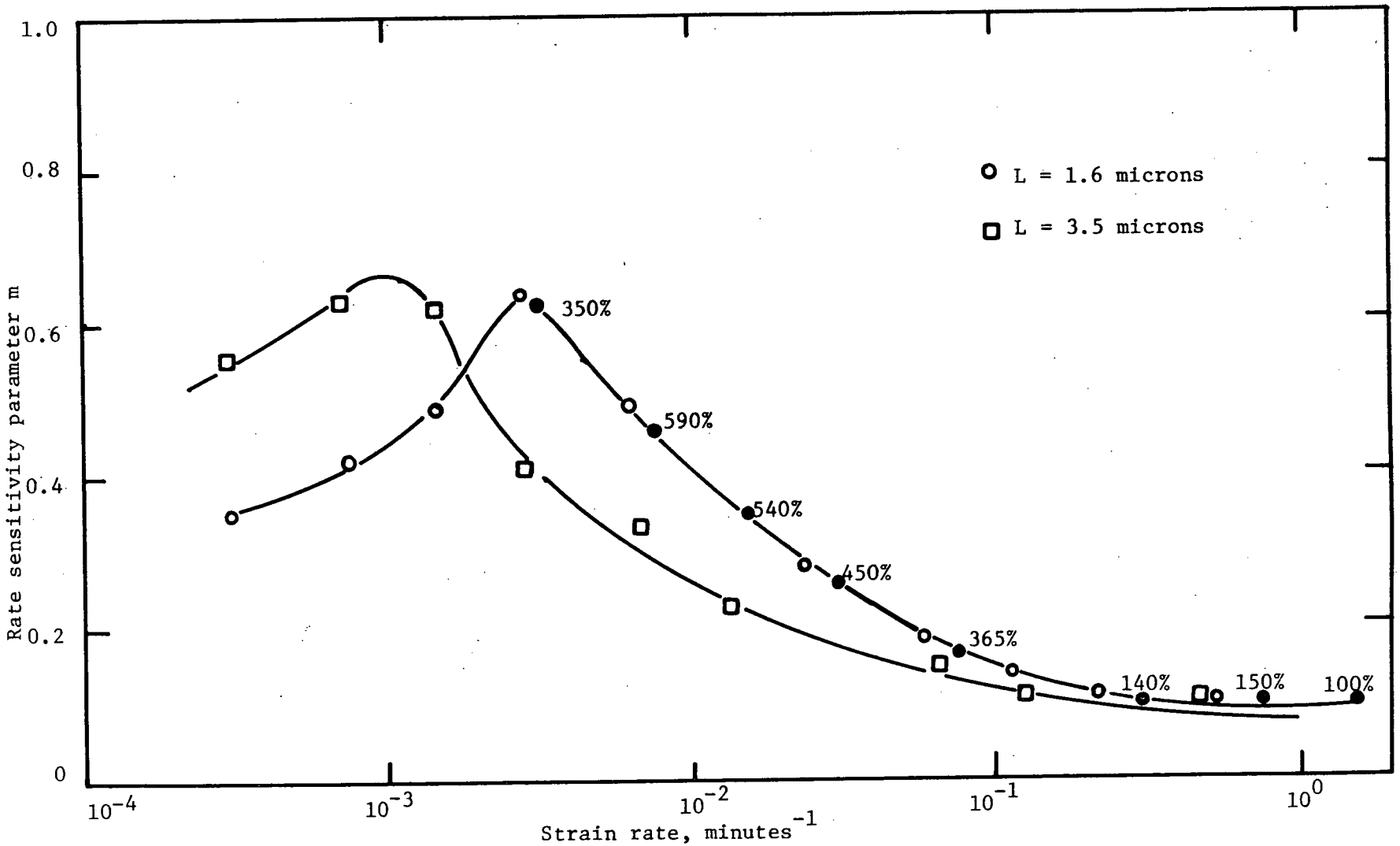

Fig. 6. The relationship between the rate sensitivity parameter m and strain rate. T = +23°C L = 1.6 microns.

observed to decrease to a value of approximately 0.1 for all grain sizes. This high strain rate value of m is typical for most metal systems when deformation is slip or twin controlled. Superimposed on the curve for the grain size of 3.5 microns are dotted circles to indicate the initial strain rates where samples were strained to failure resulting in the elongations indicated. The largest value of elongation obtained for this material was 460% at an initial strain rate of 1.5×10^{-3} min.$^{-1}$.

The results presented in Fig. 6 are for material with a smaller initial grain size (1.6 microns). Only two grain sizes were obtained in this case but the general trend suggested in Fig. 5 is consistent with the data in Fig. 6 . That is, for an increase in grain size, the region of maximum rate sensitivity is shifted to lower strain rates (from 3×10^{-3} min.$^{-1}$ to 1×10^{-3} min.$^{-1}$). There is reasonable agreement between the curve for the annealed material in Fig. 6 (L = 3.5 micron) and the curve for the as extruded material of similar grain size in Fig. 5.

Values of total elongation are again superimposed on the curve for the finest grained material in Fig. 6. The maximum value obtained was 590% at an initial strain rate of 7.8×10^{-3} min.$^{-1}$. When a specimen was deformed at a strain rate corresponding to the maximum value of m the elongation was 350%. It has been suggested[3] that the strain rates for maximum m and maximum elongation do not coincide due to the decreasing value of true strain rate as the instantaneous length increases. Thus with an initial value of m at its maximum, a decrease in strain rate results in a decrease in m and hence the material would be continually losing its resistance to necking. Correspondingly, with an initial value of m at a strain rate above the point of maximum m, the resistance to necking will be increasing as the specimen elongates.

In comparing the values of elongation to failure at high strain rates for the two grain sizes it is interesting to note that the strain to fracture is always greater for the finer grain structure even at relatively high strain rates. For example, at a strain rate of 8×10^{-2} min.$^{-1}$, the 1.6 micron material deforms 360% while the 3.5 micron material fails after approximately 100-130% deformation.

3.1.3. Effect of Temperature

The test temperature was varied from +23°C to +100°C so that the apparent activation energy of the rate controlling process could be obtained. In order to stabilize the grain size at these temperatures all specimens were held at 100°C for 15 minutes before testing at any given temperature. This treatment produced a slight increase in grain size from the as extruded value of 3.5 microns to 3.7 microns.

Incremental strain rate change tests were done at four different temperatures and the results appear in Fig. 7. As the temperature of testing increases, the flow stress-strain rate curve is shifted to the right, towards higher strain rates, and possibly down as well although this trend cannot be completely established. Thus the region of maximum strain rate sensitivity is shifted to higher strain rate values as the test temperature increases. This fact is further evidenced by examining the effect of temperature on the m-strain rate relationship in Fig. 8. A general trend is developing in this set of data as seen by the increasing value of the peak m as the temperature increases. Values for m rise from 0.57 at room temperature to greater than 0.8 at +75°C. Data for the +100°C test does not follow this trend conclusively but there is a possibility that due to the stepped nature of the m determination the actual peak value may have been straddled.

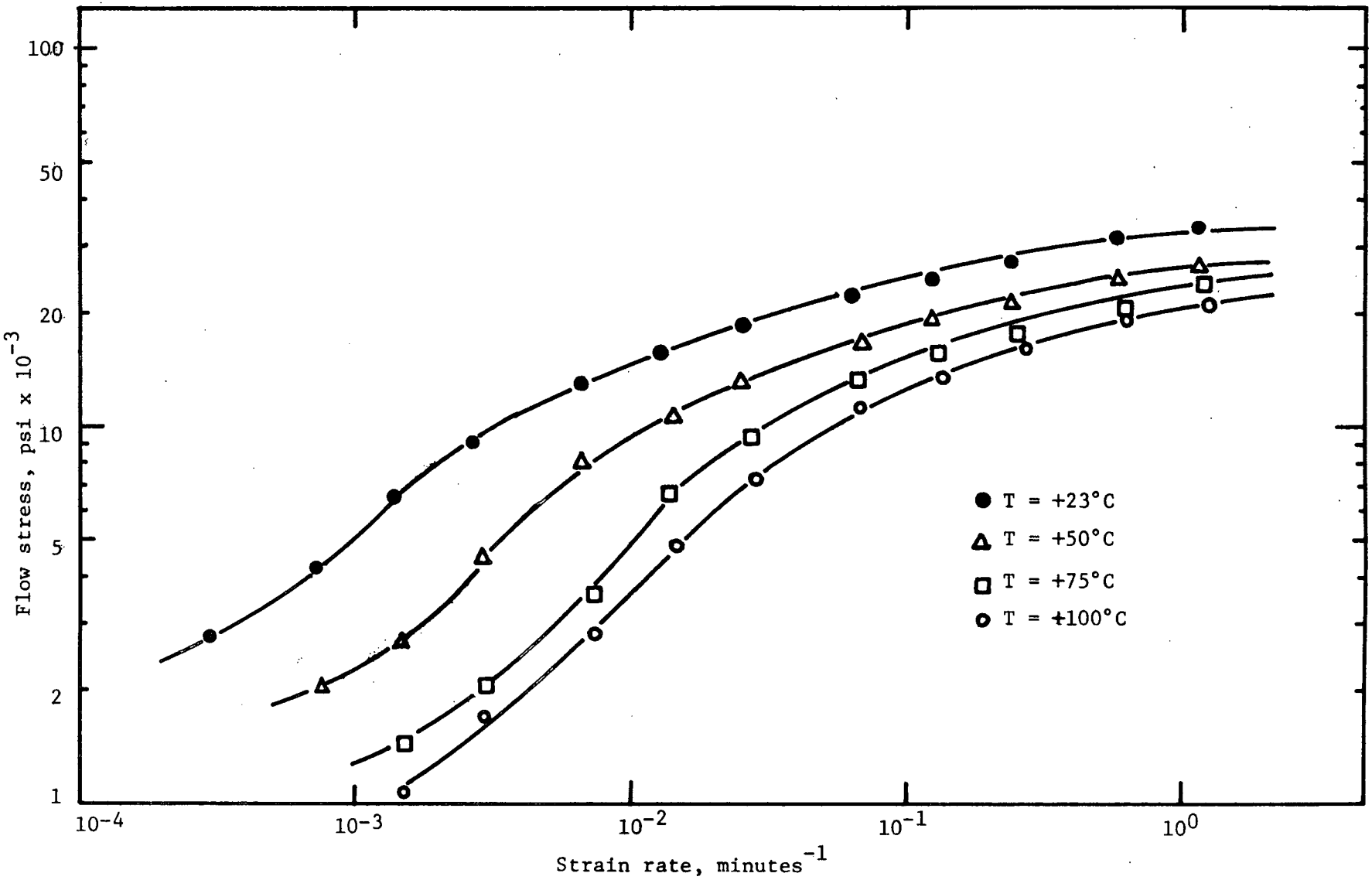

Fig. 7. The effect of testing temperature on the stress-strain rate relationship. L = 3.7 microns.

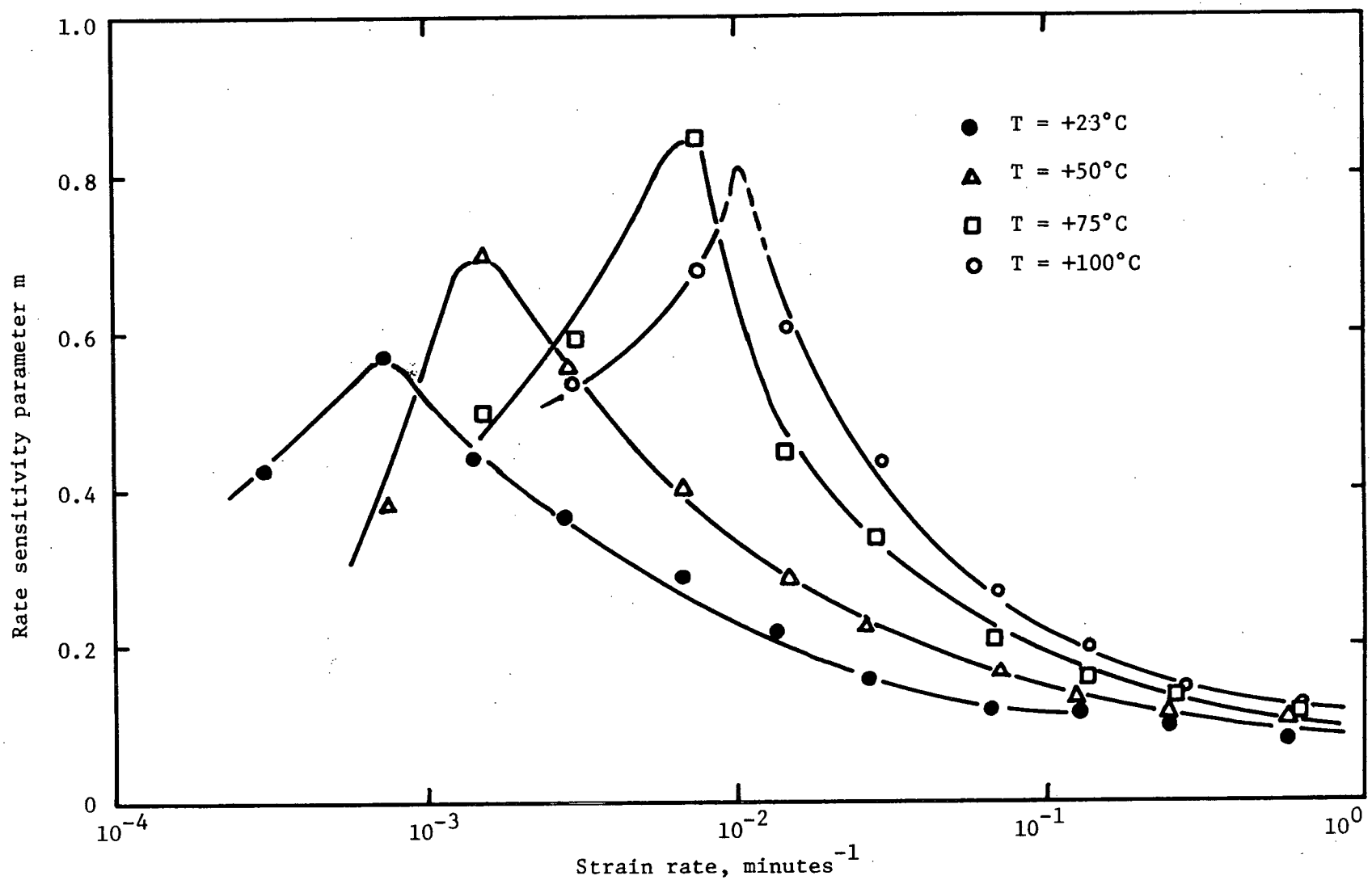

Fig. 8. The relationship between the strain rate sensitivity parameter m and strain rate at different test temperatures. L = 3.7 microns.

This suggestion is further supported by the increasing sharpness of the peak as the test temperature is increased (i.e. for 100°C. the peak m may occur at 10^{-2} min.$^{-1}$ and have a value greater than 0.85). Again, the high strain rate value for m approaches 0.1 consistent with the data on the effect of grain size (Fig. 5).

An analysis has been carried out on the data of Fig. 7 so that a value for the apparent activation energy can be calculated. This analysis is based on the assumption that the strain rate, at a constant stress, is a measure of the rate of deformation. For this calculation the values of stress selected are all in the region of high strain rate sensitivity and hence the activation energy will be associated with the mechanism of deformation in this region. The values of strain rate at various constant stresses are plotted against reciprocal temperature following the normal Arrhenius relationship:

$$\text{Rate} = Ae^{-Q/RT}$$

where A is a constant and Q, R and T have their usual meanings.

A measure of the slopes of the lines representing the data gives the value of apparent activation energy, Q, for different constant stress levels. These values are tabulated in Fig. 9 and increase from 8.3 Kcal/g.atom at 10,000 psi to 9.7 Kcal/g.atom at 3,000 psi. The activation energy for self diffusion of zinc (and diffusion of zinc in dilute Zn-Al alloys) is 20-25 Kcal/g.atom and for grain boundary diffusion is 14.5 Kcal/g.atom.[30] The value obtained in the present work, 8-10 Kcal/g.atom, is lower than that expected for a grain boundary diffusion process but the activation energy should be decreased slightly by the addition of aluminum to zinc.[30] Alden[7] has measured an apparent activation energy in the Sn-Pb system which indicates that the rate controlling process

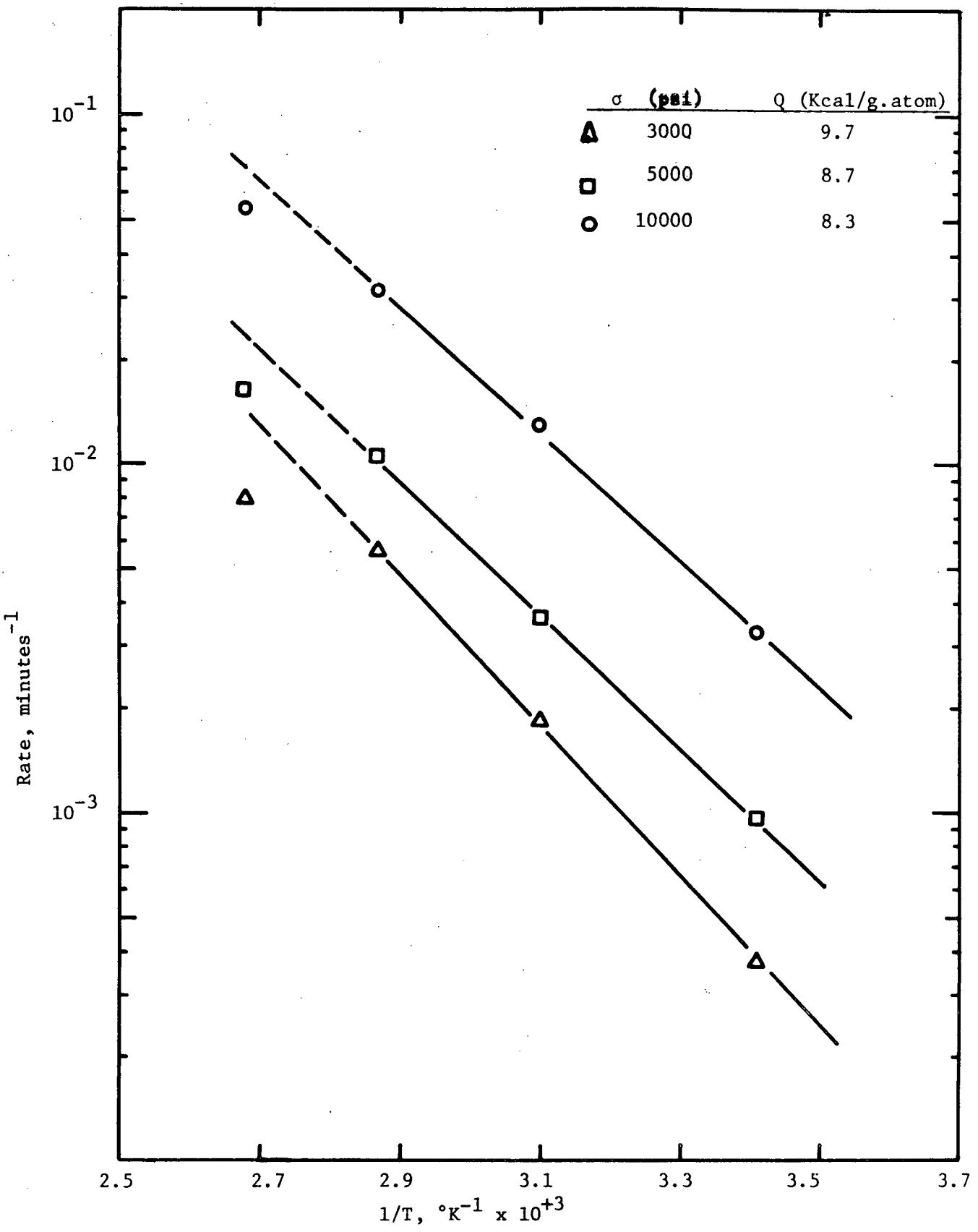

Fig. 9. Arrhenius plot for cast and extruded material. L = 3.7 microns.

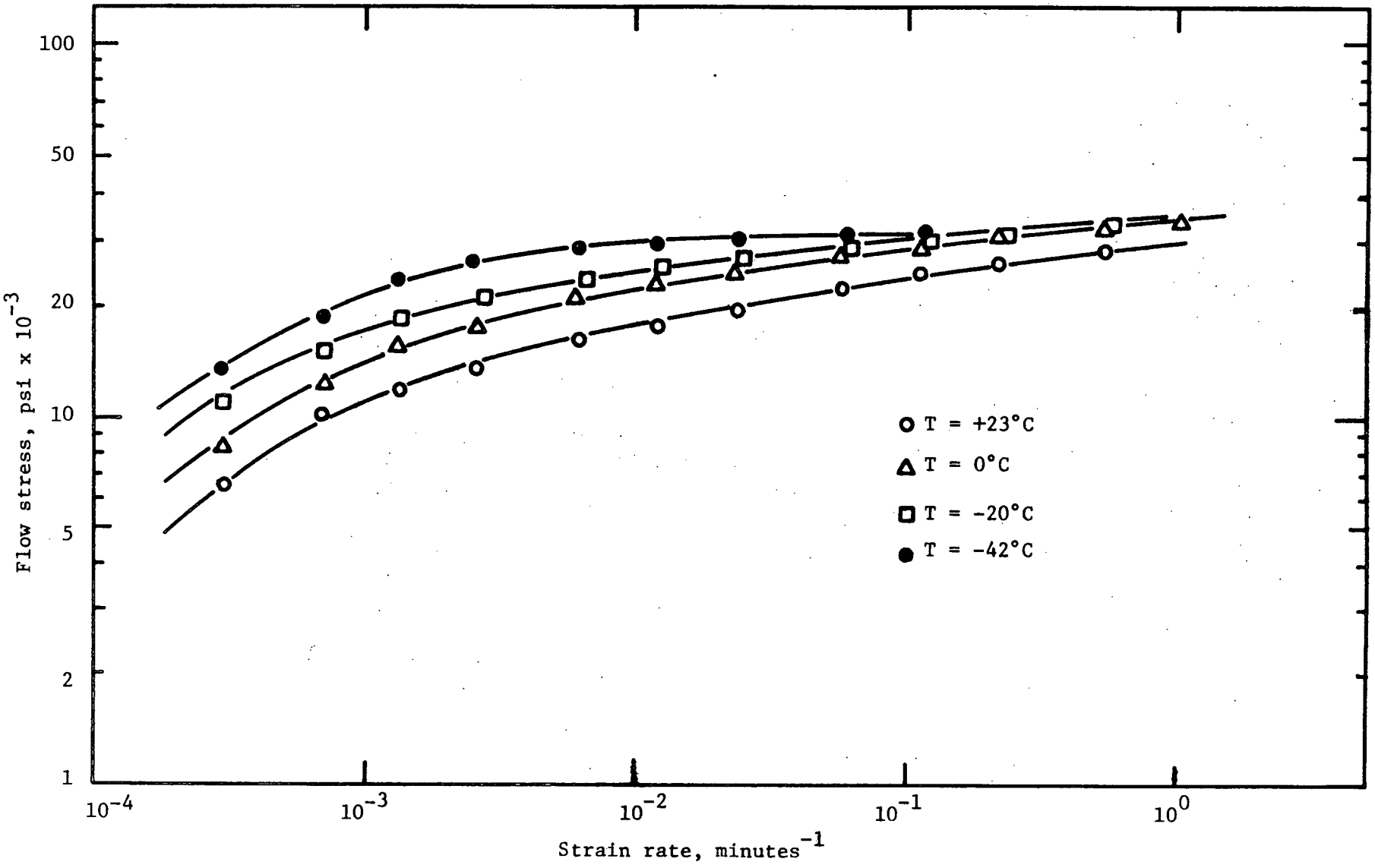

Fig. 10. The effect of testing temperature on the flow stress-strain rate relationship for pure zinc. L_o = 5 micron ± 0.5 microns.

is one grain boundary diffusion. The significance of the measured activation energy values will be discussed in more detail in a later section.

In determining the line of best fit in Fig. 9, the rate values at +100°C were essentially ignored. It is believed that the difference between these measured values and the suggested line, particularly at the low stress levels, is due to grain growth at the elevated temperature.

The effect of test temperature on the flow stress-strain rate relationship was also investigated for pure zinc extruded at room temperature (grain size $5 \pm .5$ microns). These results appear in Fig. 10 and indicate that further studies on this material would likely prove fruitless. The major difficulty arises from not being able to obtain a fine enough grain size in the high purity zinc. Although no specimens were strained to failure, the equivalent grain size in the alloy Zn-Al resulted in low values of total elongation.

A plot of m versus strain rate is not included but the results from that determination indicated that at room temperature the values of m decreased rapidly from approximately 0.4 at a strain rate of 3.1×10^{-4} min.$^{-1}$ to a value approaching 0.1 at strain rates above 3×10^{-3} min.$^{-1}$. The maximum value of m obtained decreased with decreasing test temperature to approximately 0.3 at -40°C.

3.2. Extruded Powders

3.2.1. Effect of Temperature

The effect of temperature on the flow stress-strain rate relationship was extensively examined for the extruded powder compacts and the results appear in Fig. 11. These data are consistent with the

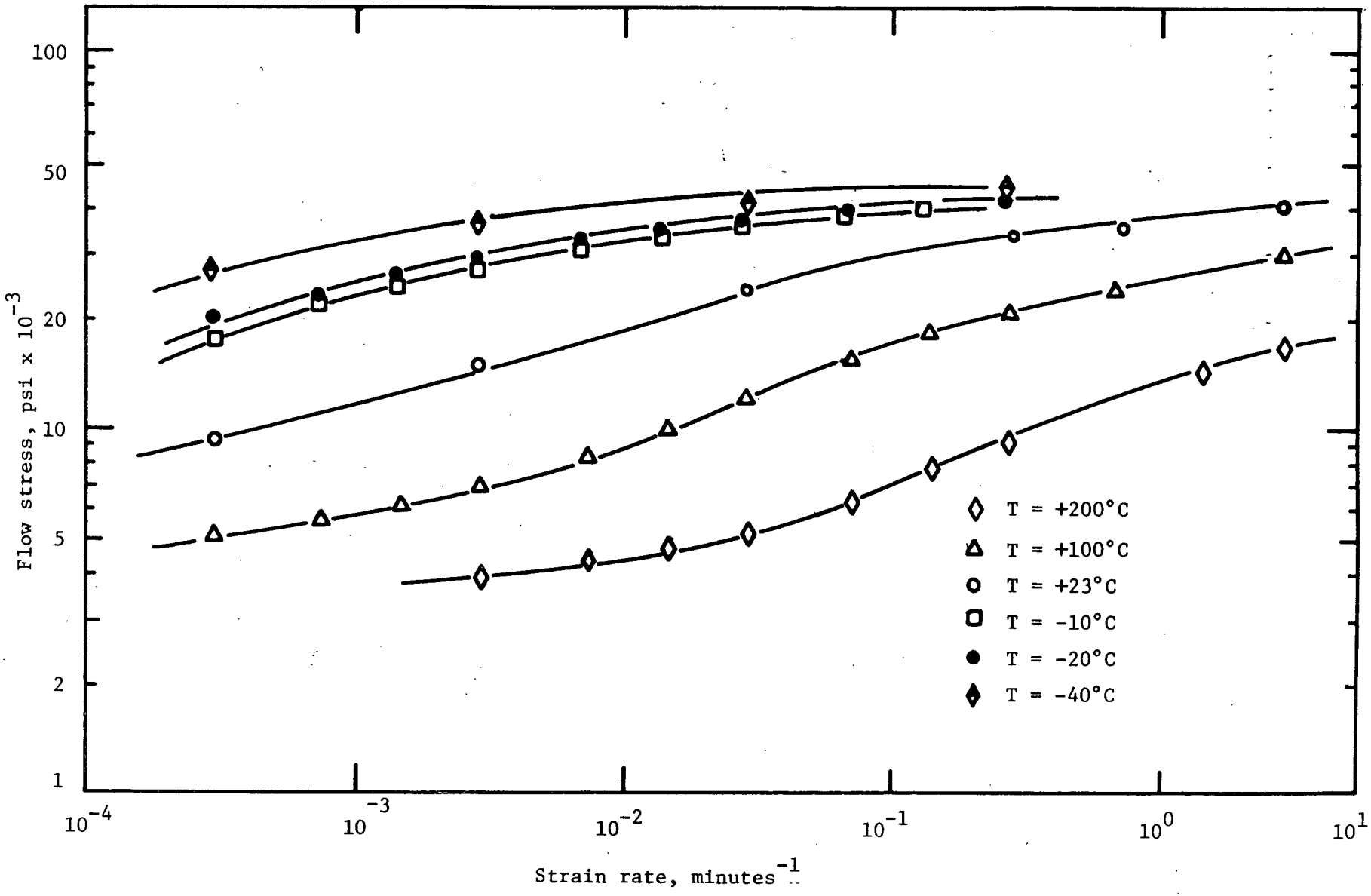

Fig. 11. The effect of testing temperature on the flow stress-strain rate relationship for extruded powder alloy. L_o = 2 microns.

previously mentioned trend which suggests that as the test temperature is increased the sigmoidal σ - $\dot{\varepsilon}$ curve is shifted down and to the right. Results for tests above room temperature reveal the entire S-shaped curve while lower temperature tests tend only to exhibit the upper portions of the highly strain rate sensitive region. At low strain rates and high temperatures the structure is relatively strain rate insensitive with the stress level approaching a value of approximately 3,000 psi. At high strain rates and low temperatures, the structure is again strain-rate insensitive with the flow stress approaching a value of approximately 50,000 psi. A comparison of these data to those for the extruded castings shows that the curves for the extruded powders may have experienced a general shift to regions of higher stress and lower strain rate (for castings low asymptote value is less than 1,000 psi and the high asymptote is approximately 40,000 psi). The most significant difference between these two sets of data is the magnitude of the measured value of m. For the extruded powders (grain size 2 microns) at room temperature the peak value for m is approximatley 0.2 (by slope estimation) at a strain rate of 3×10^{-4} min.$^{-1}$ while for the extruded castings (grain size 1.6 microns) m rises to a value greater than 0.6 at a strain rate of 3×10^{-3} min.$^{-1}$. Associated with the low value of m for the powder materials is a correspondingly low elongation to failure (less than 100% as compared to greater than 400%) at strain rates in the region of maximum m.

It is suggested that the presence of a finely dispersed oxide layer, introduced during the powder making procedure, could account for the low strain rate sensitivity and much lower elongations to failure. The presence of oxide on the grain boundaries would be expected to interfere

with a boundary shear process and hence the onset of slip would be encouraged and would be characterized by a low strain rate sensitivity parameter and a low value of total elongation.

An analysis was made of the data in Fig. 11 to measure a value for the activation energy of the rate controlling process by a procedure described earlier. Four different constant stress levels were utilized and the results appear as the usual Arrhenius plot in Fig. 12. The values for Q are also tabulated in Fig. 12 and range from 10.3 kcal/g.atom at 10,000 psi to 11.7 kcal/g.atom at 30,000 psi. The slight increase in Q as the stress level increases reflects the fact that the rates were measured in a region where the rate sensitivity is beginning to decrease which indicates that deformation is becoming increasingly slip controlled.

The values of apparent activation energy measured for this material would imply that a grain boundary diffusional process is rate controlling consistent with the earlier results for the cast and extruded alloy.

3.3. Rolled Castings

The final rolling operation on the cast billet resulted in a grain size of 16 microns. When the yield stress-strain rate behavior was studied for the as rolled material a distinct break was noticed in the $\sigma - \dot{\varepsilon}$ curve at a strain rate of 5×10^{-3} min.$^{-1}$ (Fig. 13). At strain rates above this value the stress was strain rate insensitive indicative of a slip controlled process while at lower strain rates the sensitivity increased as is typical for a grain boundary process.

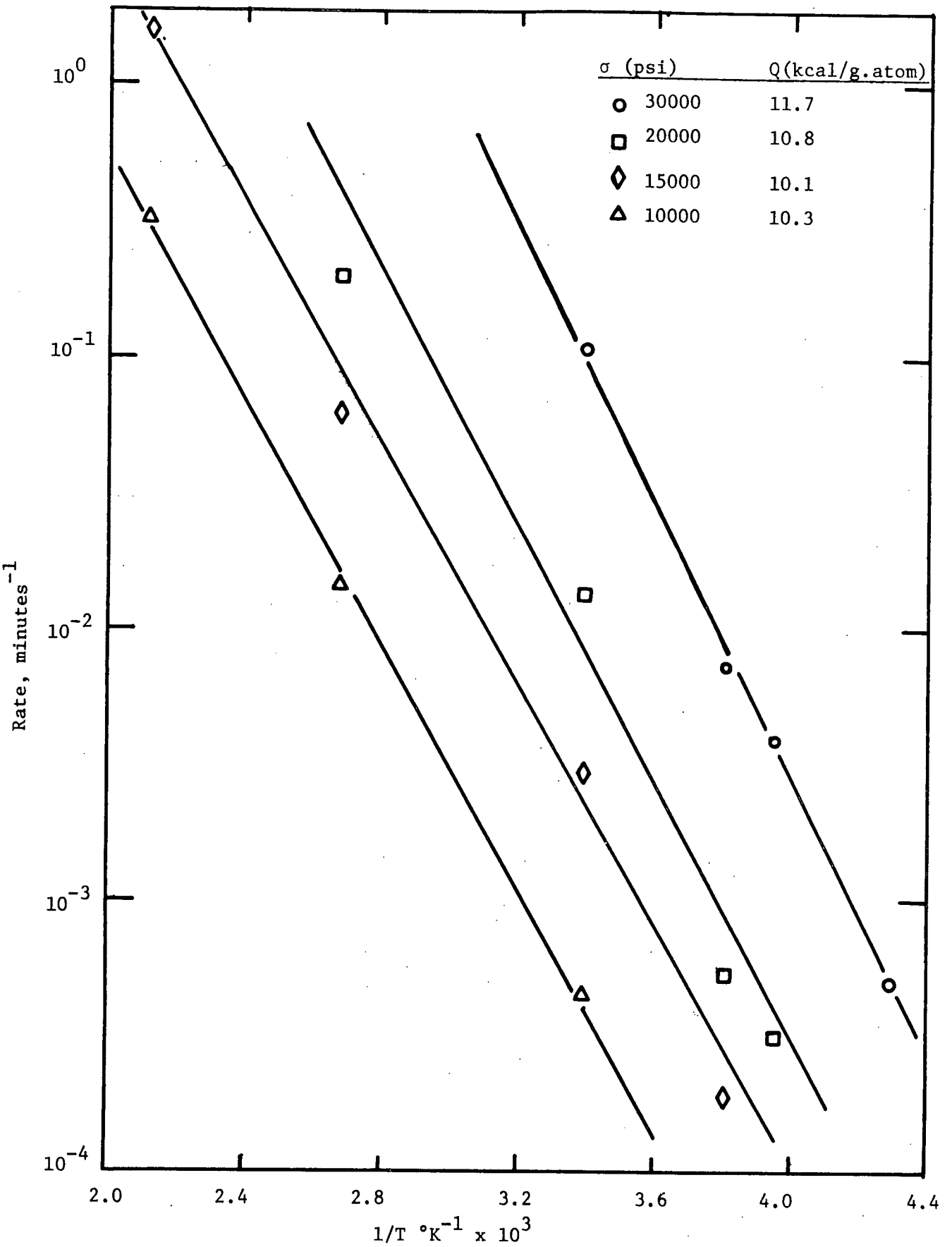

Fig. 12. Arrhenius plot for extruded powders. L = 2 microns.

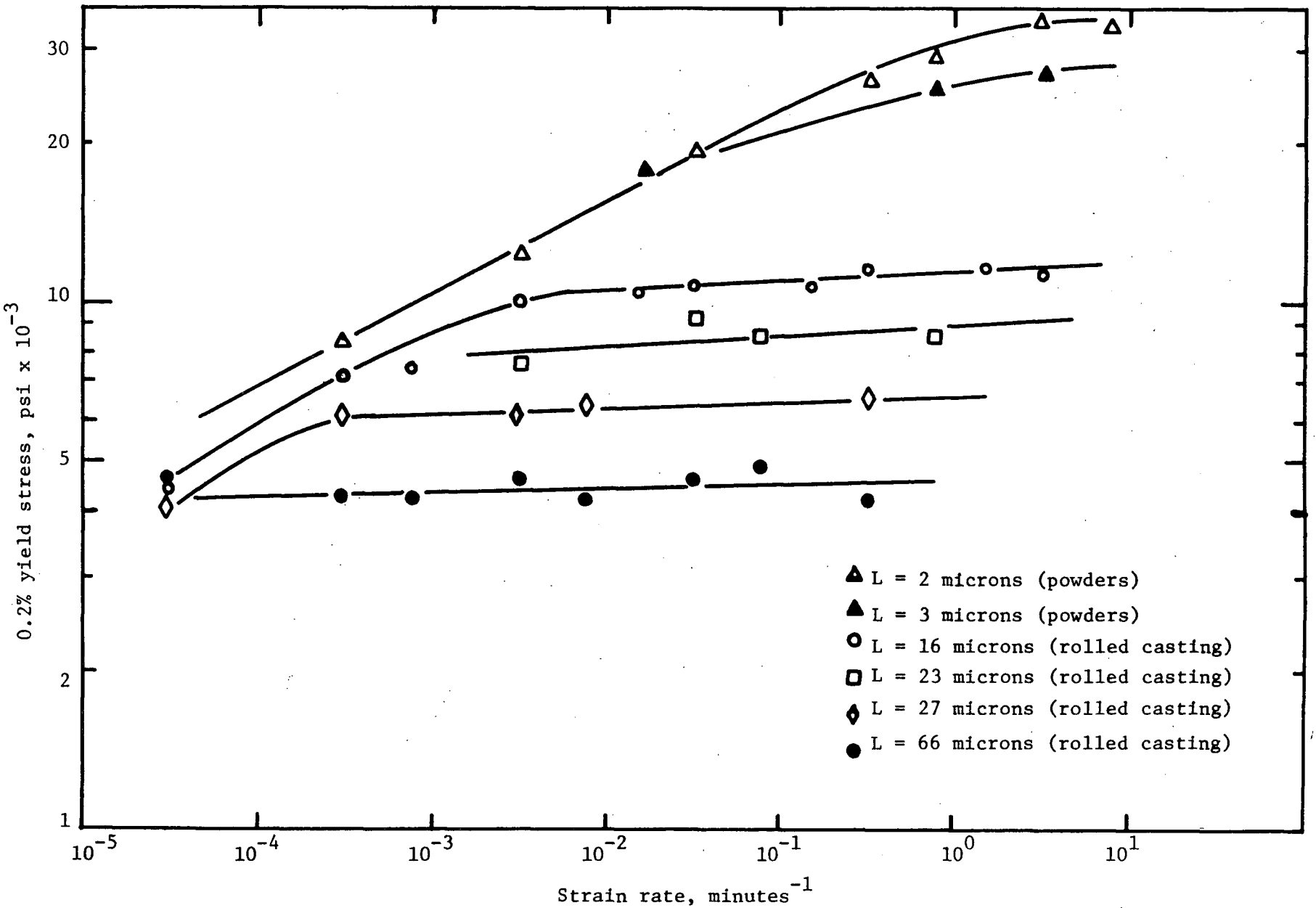

Fig. 13. The effect of grain size on the yield stress-strain rate relationship. T = 23°C.

3.3.1. Grain Size Effect

Thermal treatments as described in Table I were used to vary the grain size of the as rolled stock. The effect of changing the grain size is shown in Fig. 13 where a 0.2% offset yield stress is plotted against strain rate on logarithmic co-ordinates. Data for the extruded powders are included for comparison. In order to obtain points below a strain rate of 3×10^{-4} min.$^{-1}$ a rolled sample was machined with a gauge length of 10 times that of the normal specimen. This technique allowed values of yield strength to be obtained at a strain rate of 3.1×10^{-5} min.$^{-1}$.

Notable in the data presented in Fig. 13 is the presence of plateaus at relatively constant values of stress for different grain sizes. These plateaus dictate regions where the grain boundaries are hard and hence the deformation would be slip controlled. As the grain size is increased the plateau is shifted to lower stresses and the region of uniform stress extends to lower strain rates. For the 66 micron material the yield stress is insensitive to strain rate over the entire range sutided.

3.4. Hall-Petch Relationship

The presence of regions where the deformation is slip controlled allows a stress to be defined which should be related to the grain size through the Hall-Petch relationship:

$$\sigma_{0.2} = \sigma_o + Kd^{-1/2}$$

where σ_o and K are constants dependent on temperature and strain rate, $\sigma_{0.2}$ is the 0.2% offset flow stress and d is the mean grain boundary diameter.

The Hall-Petch plot appears in Fig. 14 and represents data from material prepared by different techniques. The large grain sizes are for the rolled and annealed material and the small grain sizes are obtained from both the extruded powders and extruded castings.

For grain sizes greater than 3 microns ($d^{-1/2}$ <0.55) all the data fit a linear Hall-Petch dependence with K approximately equal to 45,000 psi $(\text{micron})^{1/2}$. This high value of K can be attributed to the restricted number of slip systems on which deformation can occur. At grain sizes below this limit, the data for the extruded casting diverge from the linear relationship. At this grain size and strain rate the yield stress is partially controlled by grain boundary processes. To obtain the Hall-Petch value, a higher strain rate would have to be used. The data for the fine grained extruded powders remains in agreement with the Hall-Petch relationship due to boundary pinning by the oxide.

Tromans and Lund[21], in a study of grain boundary effects in Zn-ZnO alloys have measured a K value of approximately 50,000 psi $(\text{micron})^{1/2}$ at -100°C and 40,000 psi $(\text{micron})^{1/2}$ at +20°C. Their room temperature data showed a deviation from linearity below a grain size of 2 microns. It is important to note that no stress intercept (σ_o) was observed in the present work (Fig. 14). A negligible σ_o would indicate that yielding is basically controlled by slip continuity across grain boundaries and is athermal at +23°C.

3.5. Stress-Strain Curves

3.5.1. Nature of the Stress-Strain Curves

Throughout the literature many workers refer to a "steady state flow stress" which characterizes any study of superplastic materials. The inference has been that as deformation proceeds, the stress reaches

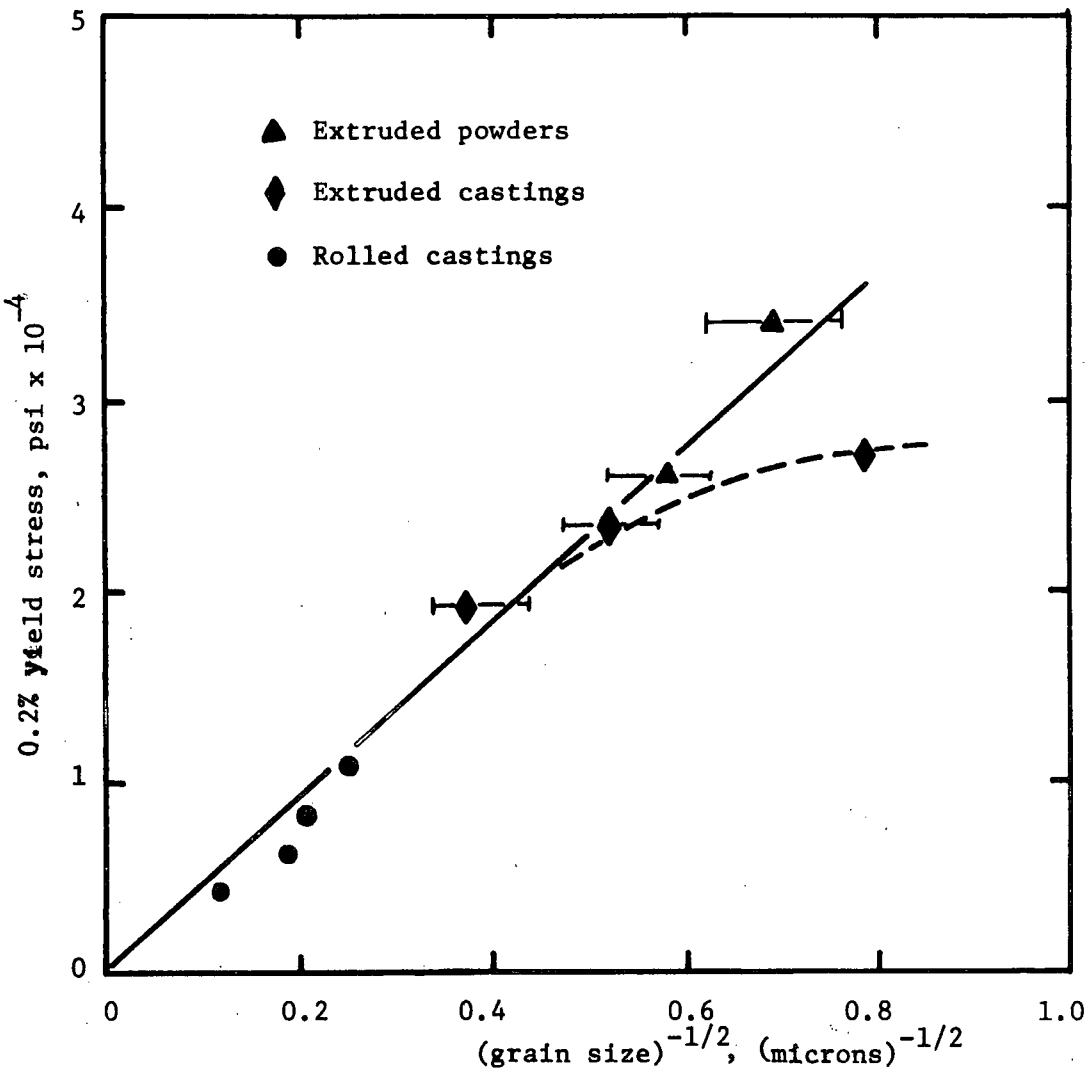

Fig. 14. Hall-Petch plot for Zn-0.2 wt.% Al. T = +23°C.

a steady state value and at the optimum strain rate extensive amounts of elongation may be obtained due to the high resistance to necking normally associated with high values of m. The "steady state flow stress" has also been important in the Backofen et al analysis of m values which involves incremental changes of strain rate after steady state conditions have been reached.[3] Thus the importance of a steady state stress has been implied and yet no where in the literature has a plot of true stress-strain appeared for superplastic materials. Plots of true stress-engineering strain are shown in Fig. 15 where the strain rate was 1.5×10^{-2} min.$^{-1}$ and the initial grain sizes were 1.6 microns and 3.5 microns. Of interest is the absence of a "steady state flow stress". The curve follows essentially a parabolic relationship up to a maximum value of stress and then is characterized by a linear decrease in stress with increasing strain until such time as a neck forms and failure occurs. The effect of increasing the grain size is to shift the peak value of stress to lower strains and higher stresses.

Any analysis of superplasticity is difficult because of the continual decrease in specimen strain rate during deformation (when a constant crosshead machine is used). For the curves in Fig. 15 the strain rate decreases from an initial value of 1.5×10^{-2}min.$^{-1}$ to approximately 3×10^{-3} min.$^{-1}$ at 500% elongation. Hence, a possible explanation for the linear decrease after the peak stress could be the decrease in strain rate. The implications of the suggestion will be discussed later.

3.5.2. Microstructural Changes with Increasing Strain

The appearance of the true stress-strain curve in the region up to the maximum stress was different from that implied in the literature in that after initial yielding occurs, rapid hardening is observed up to

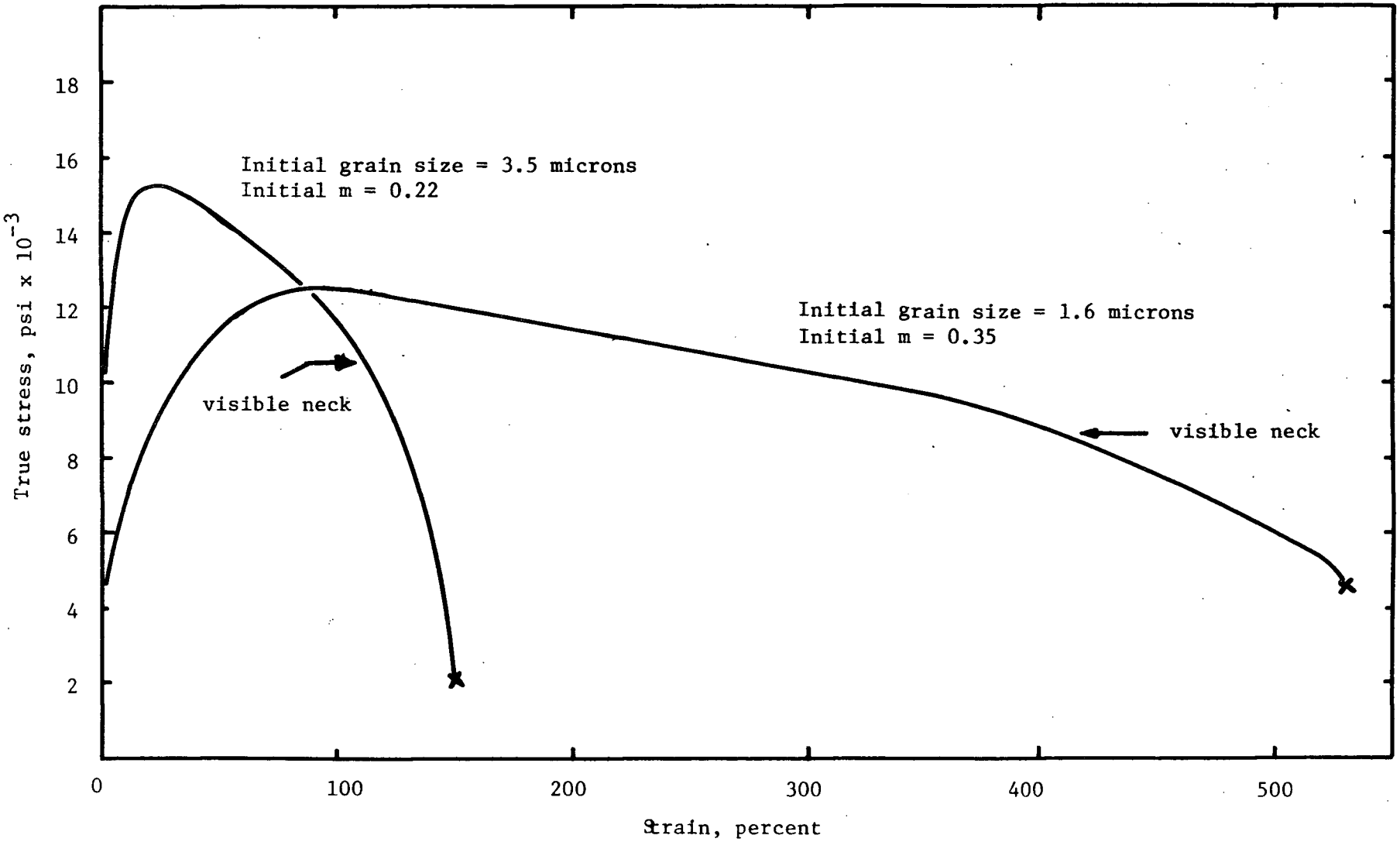

Fig. 15. True stress-strain curves for specimens of different initial grain sizes. T = +23°C $\dot{\varepsilon}$= 1.5 x 10^{-2} $min.^{-1}$.

approximately 100% strain. Several workers have reported that deformation appeared to encourage grain growth and Alden[6] suggested that an increasing stress during testing reflected the increasing creep resistance of larger grained material. The assumption that grain growth would occur, particularly in a dilute alloy system, formed the basis for a study on the effect of strain on the microstructure. Specimens were polished and observed under polarized light to determine the initial grain size and then deformed to various strains. Following the deformation, two stage carbon replicas were taken from the deformed surface and observed on a Hitachi 100 KV electron microscope. The grain size after deformation was determined by repolishing and observation under polarized light. The results of the tensile tests are shown in Fig. 16 and are reproducible to $\pm$6%. The table in Fig. 16 showing the grain growth as a function of strain also includes the grain size of a specimen strained to the maximum elongation obtained at an initial strain rate of 7.8×10^{-3} min.$^{-1}$.

The effect of increasing strain on the microstructure is illustrated in Fig. 17. The degree of grain boundary shear is greater after 43% strain than after 11%. Slip lines are observed on the larger grains in Fig. 17b. Optical micrographs on the repolished surfaces of these specimens indicated that the average grain size had increased from 2.7 microns at 11% strain to 3.3 microns at 43% strain.

An examination at higher magnification (Fig. 18) showed that slip traces completely traversed the old shear markings associated with the prior grain size and terminated only on boundaries which were characteristic of the larger grain size. This observation is consistent with the argument for a non-continuous grain growth process. It is observed that the large grain illustrated in Fig. 18 originally consisted of up to eight grains of size comparable to the initial grain size.

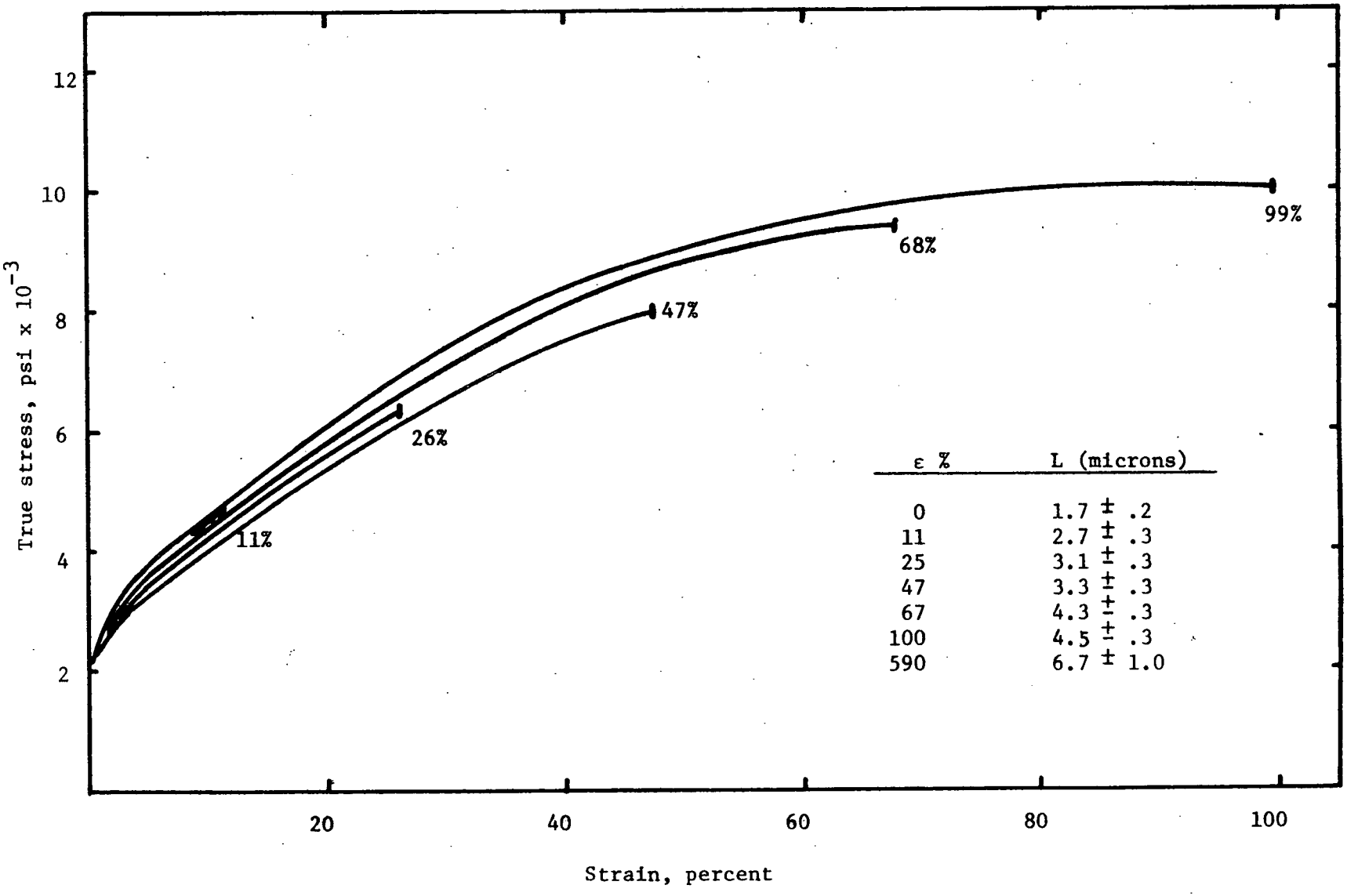

Fig. 16. True stress-strain curves for specimens subjected to different strains. T = +23°C, $\dot{\varepsilon} = 7.8 \times 10^{-3}$ min.$^{-1}$.

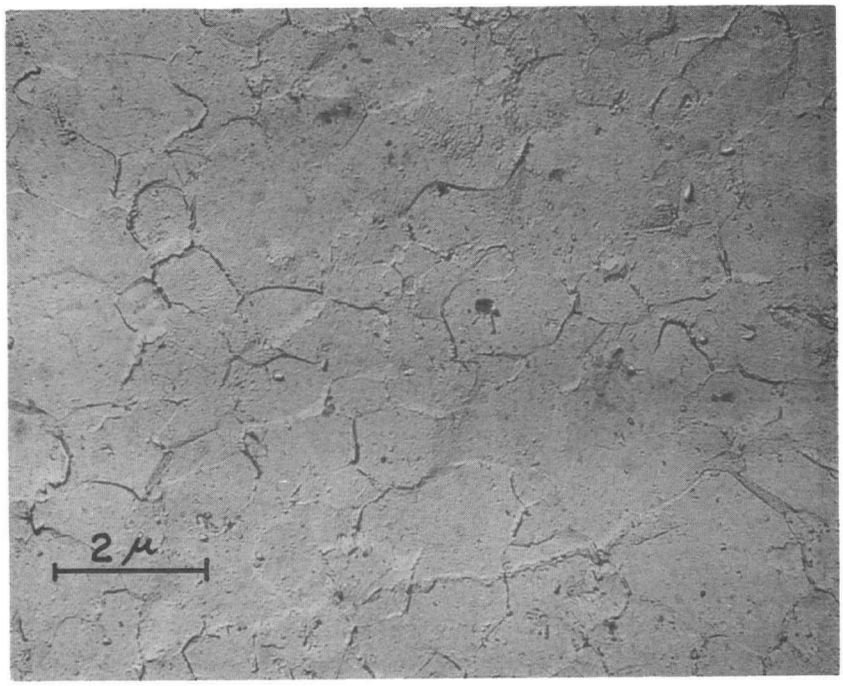

a) 11% strain

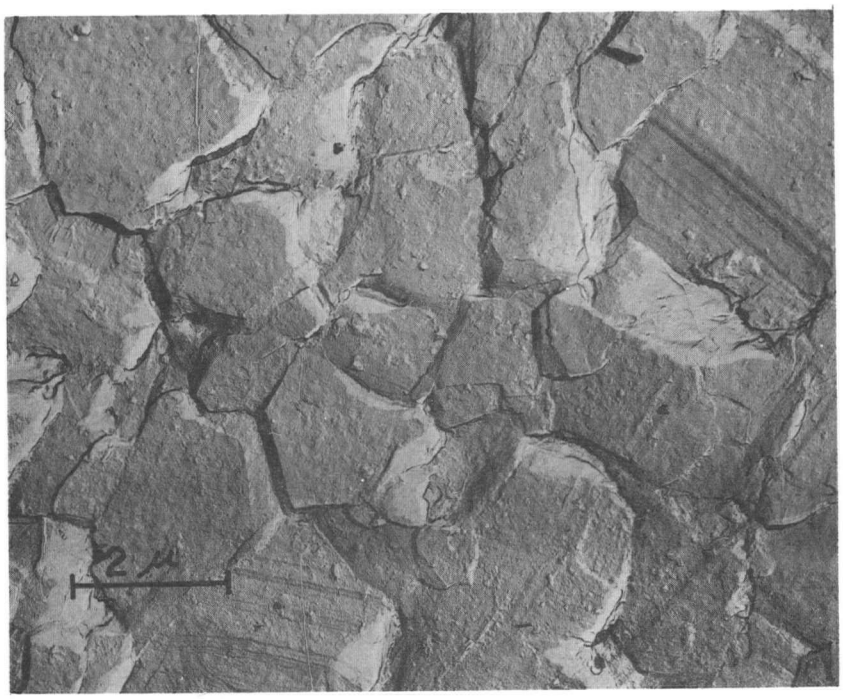

b) 43% strain

Fig. 17. Surface deformation characteristics at different strains. $T = +23°C$, $\dot{\varepsilon} = 7.8 \times 10^{-3}$ min.$^{-1}$, $L_o = 1.6$ microns.

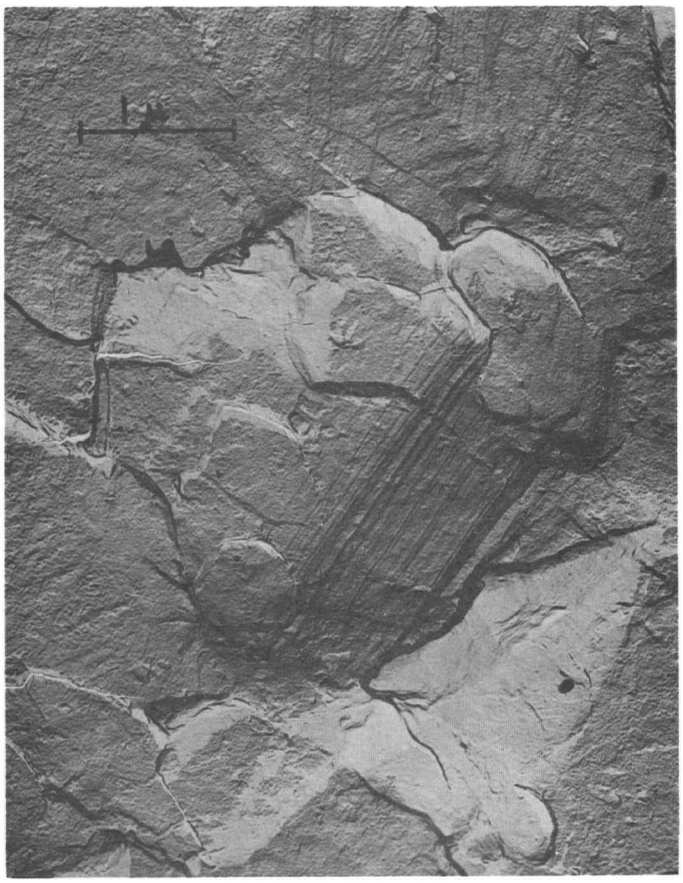

Fig. 18. Slip traces at 43% strain. T = +23°C, $\dot{\varepsilon} = 7.8 \times 10^{-3}$ min.$^{-1}$, L_o = 1.6 microns.

Fig. 19. Grain boundary shear and grain rotation at 43% strain. $T = +23°C$, $\dot{\varepsilon} = 7.8 \times 10^{-3}$ min.$^{-1}$, $L_o = 1.6$ microns.

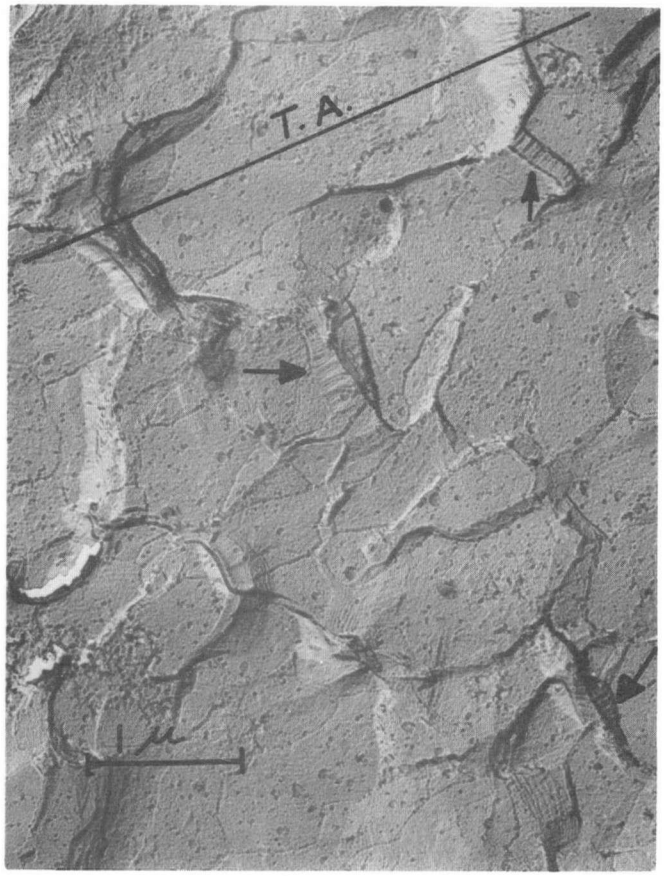

Fig. 20. As strained surface showing striated bands (marked by arrows) in grain boundary regions at 43% strain. $T = +23°C$, $\dot{\varepsilon} = 7.8 \times 10^{-3}$ min.$^{-1}$ $L_o = 1.6$ microns.

The extensive amount of grain boundary shear is also observed in Fig. 19 where a longitudinal scratch has become offset in the region of the boundary. Grain rotation has also occurred during the deformation as demonstrated by the different directions that the scratch has assumed within each of the three grains illustrated.

The last of the electron micrographs (Fig. 20) illustrates striated bands along several tensile loaded boundaries. In this micrograph, the tensile axis is shown by the line inclined approximately 20° from horizontal. In the Pb-Sn eutectic system, Zehr and Backofen[11] recently observed striated regions similar to those in the present work and they suggested that this banding is metallographic evidence for the occurrence of a diffusional creep process.

Also visible in Fig. 20 are the networks of old grain boundaries within the larger grained final structure. The amount of shear on these original boundaries is minimal in comparison to that on the final boundaries indicating that the grain size has changed rapidly in the initial stages of deformation resulting in a larger contribution to total strain coming from shear on the boundaries of the larger grains.

The grain size dependence on strain is shown in Fig. 21 on logarithmic co-ordinates. The degree of deformation is plotted in terms of both engineering (solid) and true strain (dotted). Lines of best fit are drawn through the points ignoring the zero percent strain condition. It may be argued that data obtained at very low amounts of deformation would not be expected to follow the linear relationship since a finite amount of boundary shear is required to initiate the grain growth process. Thus if one assumes that the grain size would remain stable up to an arbitrary

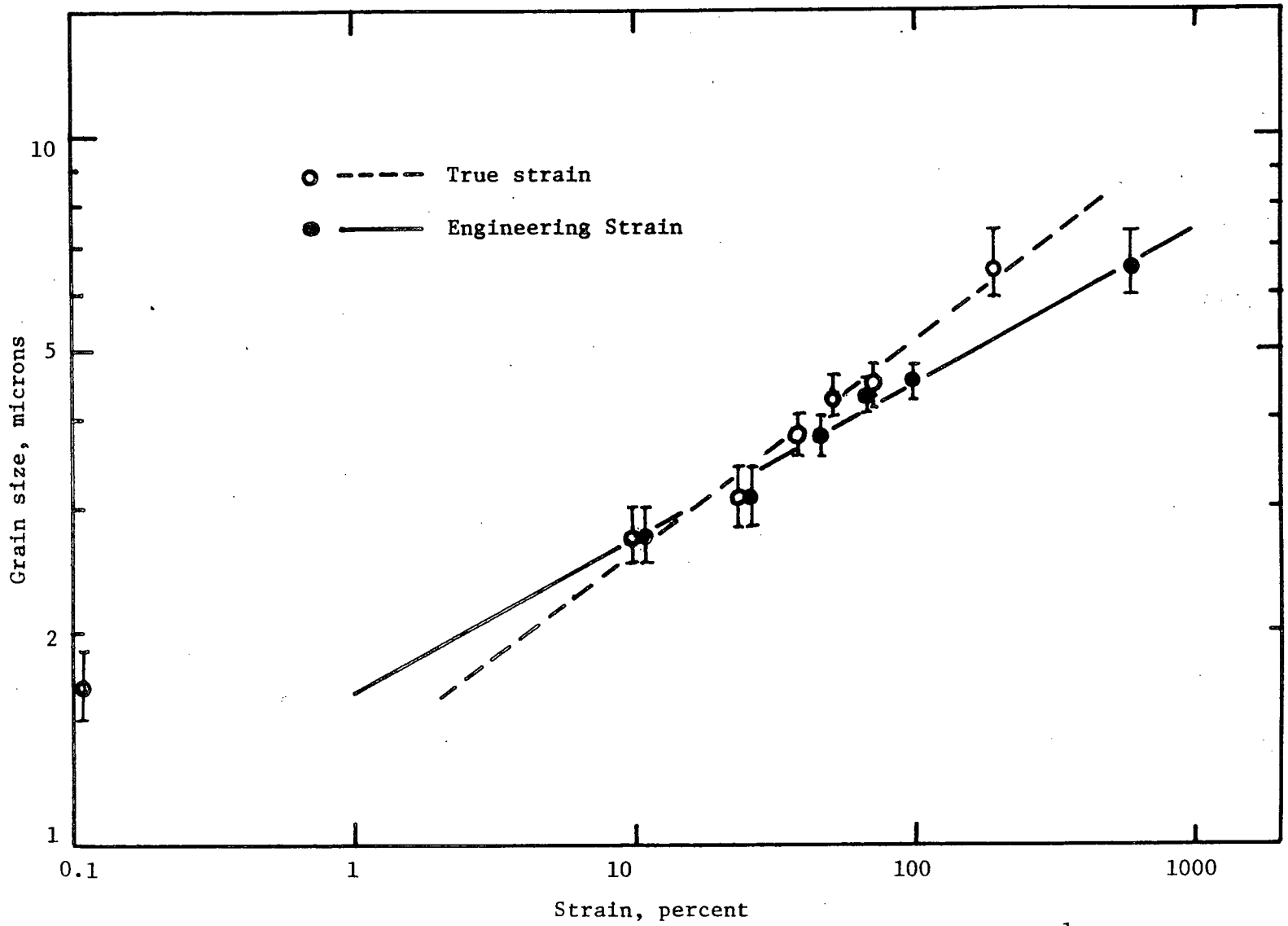

Fig. 21. Dependence of grain size on strain. T =+23°C, $\dot{\varepsilon}$ = 7.8 x 10^{-3} $min.^{-1}$.

value of 1 or 2% strain then all the data lie on the illustrated relationships.

3.5.3. Strain Rate Dependence of True Stress-Strain Curves

In the present work the effect of strain rate on microstructure was not examined in detail. However the true stress-strain curves at a few different strain rates appear in Fig. 22. The grain size of the cast, homogenized and extruded material was 3.2 microns. The effect of increasing the strain rate is to shift the peak value of stress to lower strain values (Table II).

TABLE II

The dependence of strain to maximum stress and initial m on imposed strain rate

Strain Rate ($min.^{-1}$)	Strain to Maximum Stress (%)	Initial m
.002	100	.72
.008	48	.54
.02	34	.38
.04	22	.30
.08	15	.24
.2	15	.20

It is not known how the strain rate affects the rate of grain growth during deformation as this study was restricted to a single strain rate. However, the above results suggest that grain growth may be a sensitive function of strain rate and hence be an important parameter in superplasticity as will be discussed later.

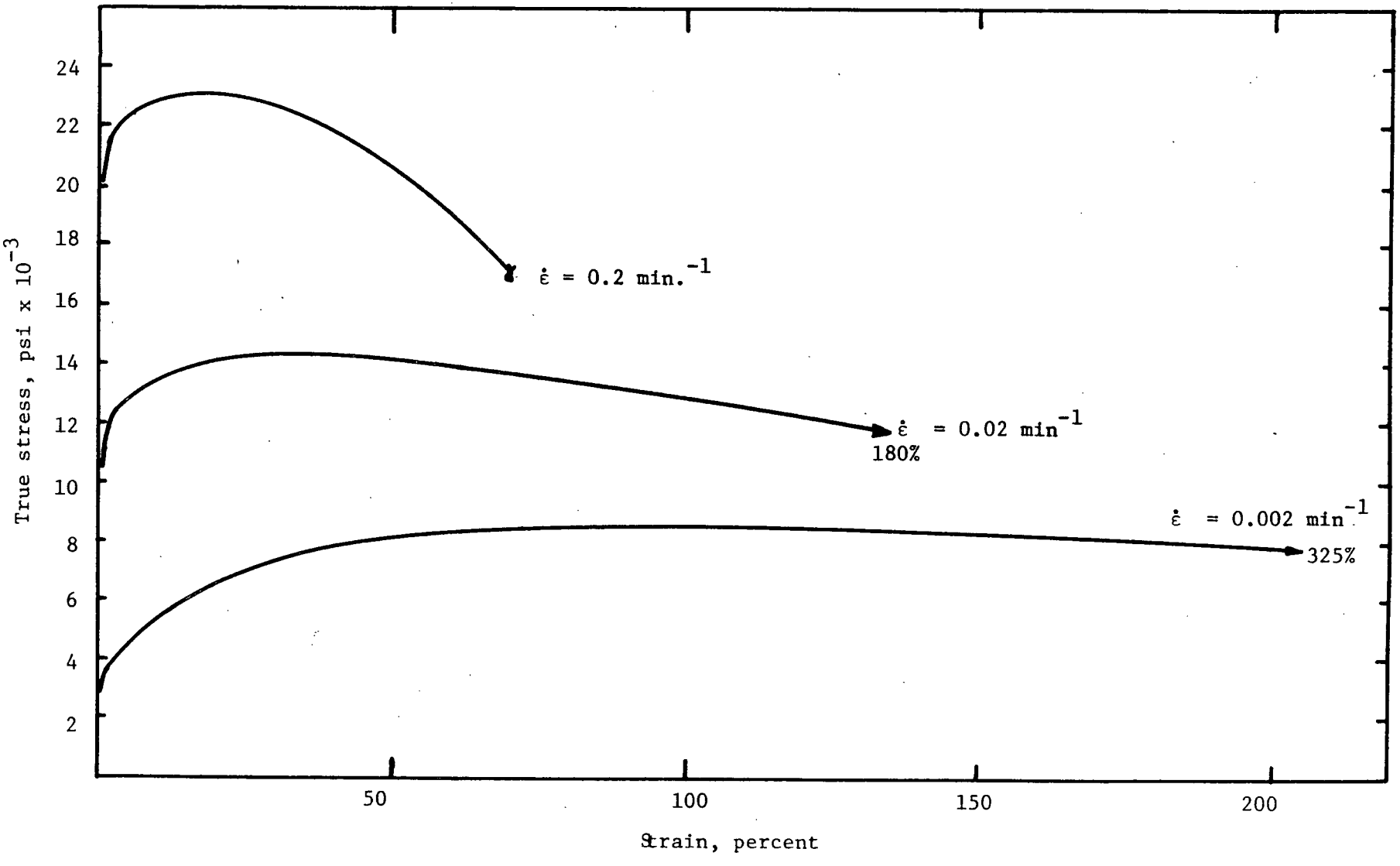

Fig. 22. True stress-strain curves for cast and extruded material. T = +23°C, L = 3.2 microns.

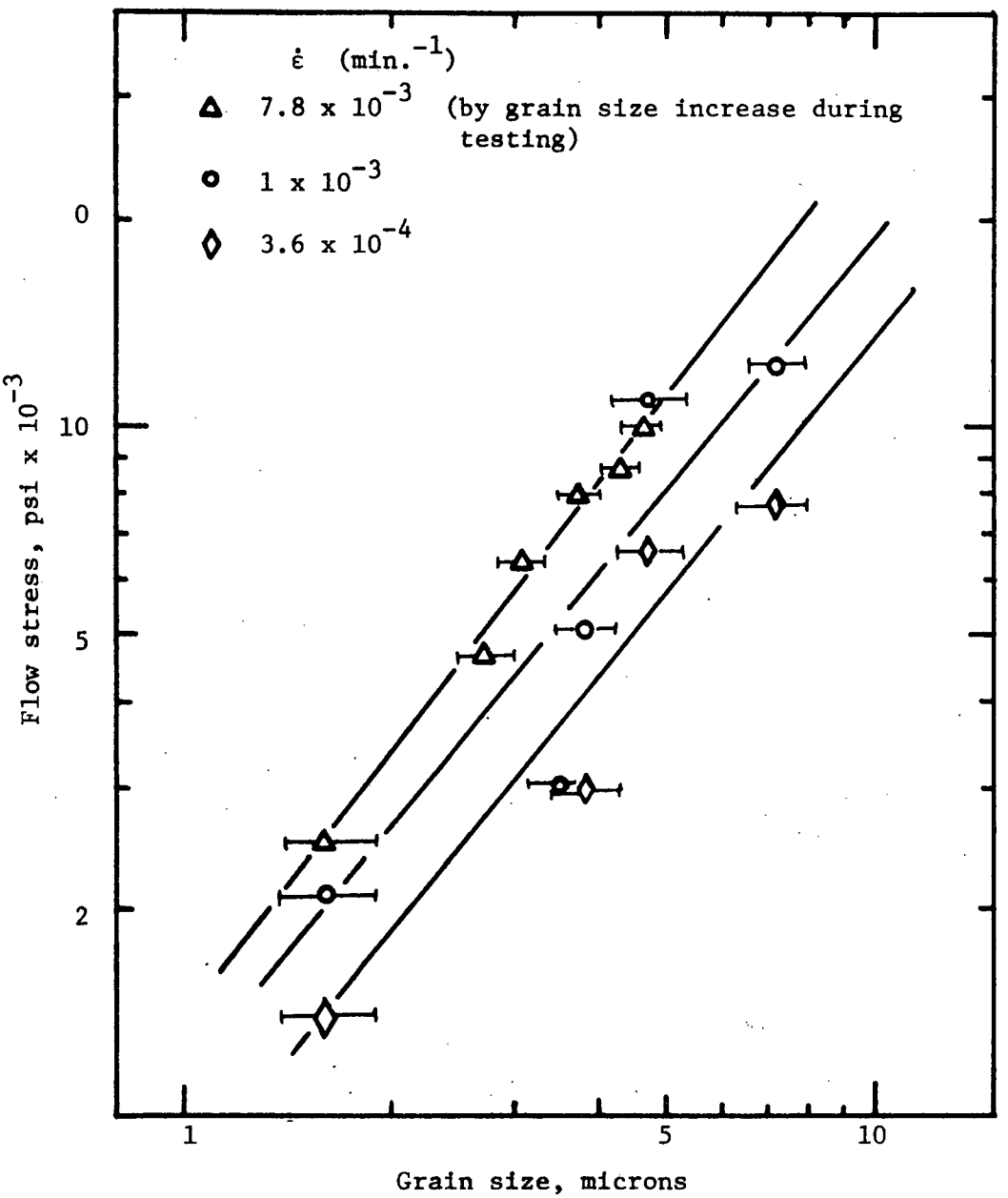

Fig. 23. Dependence of stress on grain size at various strain rates. T = +23°C.

In the absence of deformation, no detectable grain growth occurs in a period of time comparable to the testing time.

3.5.4. Effect of Grain Size on Stress During Deformation

By cross plotting the data from Fig. 4 at various constant strain rates against grain size on logarithmic co-ordinates, the stress dependence on initial grain size may be determined. Such a plot is shown in Fig. 23. The data for the two lowest strain rates have been taken from Fig. 4 but the data for the highest strain rate (7.8×10^{-3} min.$^{-1}$) originated from Fig. 16 where the grain size was actually measured at various strains. The scatter at the lower strain rates is much larger since the effect of strain has been ignored in plotting the grain size.

The similar nature of the relationships shown in Fig. 23 indicates that the flow stress may be related only to instantaneous grain size irrespective of the origin of the structure. It can then be assumed that the observed hardening demonstrated by the true stress-strain curves (Fig. 15 and 16) is due only to the increase in grain size during deformation.

Since the most reliable data presented here relates to the actual measured grain size during deformation ($\dot{\varepsilon} = 7.8 \times 10^{-3}$ min.$^{-1}$) the grain size dependence on stress may be represented by the relationship:

$$\sigma \propto d^{1.3}$$

In similar plots, other workers have measured the value of this exponent to be between 1 and 3 depending on the system under investigation and the techniques used to evaluate this dependence. All previous techniques have been restricted to cross plotting data obtained from the stress-strain rate dependence on grain size. Hence, the present technique should be more reliable in determining a true effect of grain size on stress.

4. DISCUSSION

4.1. Significance of the Strain Rate Sensitivity Parameter

The phenomenological basis for superplasticity is the strong dependence of the observed flow stress on the imposed strain rate. As a result the concept of a strain rate sensitivity parameter m has been invoked to describe this behavior. The parameters which are known to affect the initial value of m are strain rate, temperature, amount of second phase present and grain size. Thus any study of superplasticity has been concerned with the behavior of m when any one of these parameters are varied while the others are held constant. However the ideality of this situation is disturbed by several factors which are present under many testing conditions. The most obvious is the variation of strain rate resulting from the change of specimen length during an elongation to failure investigation where the final length may be greater by a factor of ten than the initial length. Some workers have attempted to alleviate this problem by increasing the crosshead motion during a long term test to offset the effect due to increasing gauge length. However the only real solution is to carry out testing on apparatus which allows a continuous variation of crosshead speed such that a true constant strain rate may be achieved.

In the present study, observations of an increasing grain size during testing present yet another variable parameter which has normally been assumed to be a constant. Thus in any system where grain growth is encouraged by deformation a discussion of m must include not only the effect of established parameters but also the effect of strain on the grain size. It should be noted that the variation of m with strain rate, for example Fig. 5 and Fig. 8, is valid only for the initial structure since the total strain involved is small with respect to the maximum

possible elongation and the amount grain growth is correspondingly low. The effect of increasing grain size becomes a problem when a discussion undertakes to explain the high degrees of elongation obtained on the basis of data pertaining to the initial structure. In particular, a description concerning a strain rate where a maximum value of m is observed loses its significance when grain growth is involved. Although the effect of grain size on the m vs strain rate relationship has been fairly well established the more important factor of the rate of change of grain size (and therefore m) with strain, strain rate and amount of second phase is unresolved. This suggestion supports the statements of Floreen[27] regarding the extent of the elongations observed in pure Ni. It was proposed that the high rate of change in grain size during testing limited the total obtainable elongation and the amount of strain which was observed had occurred while the grain size was small.

Thus to completely establish the significance of m an experimental procedure must be followed in which the variation of m is studied as a function of strain, strain rate and temperature. This could be achieved by straining a material at a constant temperature and strain rate and then conducting an m determination as previously described[3] at different values of strain.

An investigation was carried out on the change of m with strain utilizing the stress-strain curves in Fig. 22. A specimen was deformed 220% at a strain rate of 2×10^{-3} min.$^{-1}$ followed by incremental strain rate changes to determine a value of m. This value was measured to be 0.39 (initial m was 0.72). If one assumes that the linear decrease in stress with increasing strain (Fig. 15 and 22) is entirely a response to a decreasing strain rate then a strain rate sensitivity parameter may be calculated from the observed slope following the relationship:

$$m = \frac{\partial \ln \sigma}{\partial \ln \dot{\varepsilon}}$$

This analysis applied to the data for a strain rate of 2×10^{-3} min.$^{-1}$ resulted in a calculated value of 0.32 for the strain rate sensitivity parameter. This is slightly lower than the observed value of 0.39. This is due to the fact that it has been assumed that the flow stress in this region of the curve would normally be constant if the strain rate could be held constant in the specimen. However, it has been shown that even at these high amounts of strain the grain size is still increasing slightly with strain. Therefore the true stress should still be increasing under conditions of constant strain rate. Therefore the numerator of the above expression has a slightly lower value than under steady state conditions. However the general idea of the decrease in stress being due only to the decreasing strain rate is still valid.

4.2. Implications of Mechanism

As suggested earlier, any discussion of mechanism should draw support not only from tensile behavior but also from metallographic observations. Activation energy measurements have resulted in values of approximately 10 kcal/g.atom for both the extruded powders and extruded casting. Although one material behaves superplastically while the other does not the same measured value of apparent activation energy in no way implies an inconsistency since it is the rate controlling process which gives rise to the observed activation energy. The absolute value of the rate at which the reaction occurs is different but the rate controlling process is the same (ie. similar slopes on an Arrhenius plot).

Previous work on superplastic systems has proposed that assuming the stress-grain size dependence follows the relationship $\sigma \alpha L^a$, a measured value of a = 1 would imply a process of grain boundary shear, while values of 2 or 3 would be indicative of Nabarro-Herring creep or the Coble variant for grain boundary diffusional creep[8]. The value of a = 1.3 from Fig. 23 is consistent with a grain boundary shear process but the question of the validity of this type of analysis is unresolved.

Observations of grain growth during deformation have been made in many systems[6,7,9,11,18,27] but have generally been ignored in an ensuing mechanistic discussion. The nature of grain growth in the present work has resulted in the following characteristics:

a) Grain growth is greatly enhanced by deformation (table in Fig. 16 and Fig. 17).

b) Grain growth is a discontinuous process. A gradual increase in grain diameter would result in ledges forming due to consecutive shearing and migration processes, while a sudden increase in grain size would be expected to result in a surface structure similar to Fig. 18 or Fig. 20, where the shear markings delineating the original structure resemble a network of subboundaries.

c) Grain growth is rapid during the initial stages of deformation but tends to decrease as strain increases (Fig. 21).

Based on these observations, a model incorporating grain boundary shear and "explosive grain growth" is proposed to account for the superplastic behavior of this alloy. Shear on the original boundaries is assumed to occur initially and since this process is essentially one contributing to hardening, a driving force for grain boundary migration is created due to differences in dislocation density on either side of

a shearing boundary. This difference in density could result from sources first becoming operative in the larger grains of the matrix (from slip plane length considerations) leading to a greater density of dislocations being supplied to a boundary from within a larger grain. Hence, following shear by a climb-glide or similar mechanism, the boundary moves rapidly to eliminate the areas of highest dislocation density. Therefore, the larger grains tend to decrease in size as the smaller grains grow - a suggestion consistent with observations of an equiaxed structure after large amounts of superplastic deformation.

The observation of a linear logarithmic dependence of grain size on strain (Fig. 21) is not completely understood. The problem is complicated by a continually decreasing strain rate which may or may not affect the rate of grain growth. At present it is thought that a decrease in the explosive nature of the proposed boundary migration may result in the fluctuation of boundaries back and forth to eliminate alternate layers of excess dislocations.

Although no conclusive evidence for this type of behavior has been observed, a small degree of support is found on numerous electron micrographs of replicas taken from the deformed specimen surface. In particular, some boundary regions are broad, wavy and diffuse in nature which may indicate that their origin was from some process other than a simple shearing. The possibility also exists that the striated regions observed by Zehr and Backofen[11] as well as in Fig. 20 may well be indicative of a boundary fluctuation process rather than one of diffusional creep.

A final observation of the deformed surface microstructure is that some grain elongation had occurred at a strain rate where large

elongations are obtained. This could come as a result of the effect of a limited amount of slip combined with Nabarro-Herring creep.

It may therefore be proper to think in terms of grain boundary migration as the rate controlling process in superplasticity instead of the specific deformation modes associated with boundary shear. Although migration cannot by itself contribute to strain it can be rate controlling if it does determine the rate at which shear can occur. Any boundary motion will definitely affect the dislocation structure in the region of the boundary and hence will determine the stress-strain rate relationships. The observed activation energy of 10 kcal/g.atom is approximately that expected for diffusion in the region of a grain boundary and hence for the process of boundary migration. This value would also be expected for dislocation climb[20] (associated with shear) in the region of a boundary. Therefore any activation energy determination by itself cannot distinguish between these two known features associated with superplasticity. However the continuity of the shear mode of deformation is dependent on the migration process. Therefore it is felt that migration itself must be rate controlling.

5. SUMMARY AND CONCLUSIONS

The interpretation of the metallographic and tensile behavior observations made on the zinc-rich solid solution of the Zn-Al eutectoid alloy may be summarized as follows:

1) The extensive elongations and high strain rate sensitivity generally associated with superplastic materials have been observed in a fine-grained Zn-0.2 wt. % Al alloy at $T_H = 0.42$. This is the lowest homologous temperature at which superplasticity has been observed in any system to date.

2) The region of superplastic behavior is observed at higher strain rates as the grain size is refined. The most important requirements are a grain size in the micron range and grain boundaries that are relatively free of obstructions. Excessive amounts of oxide in the alloy tend to interfere with grain boundary shear and migration, and thus restrict superplastic deformation.

3) Considerations of the strain rate sensitivity determinations at large amounts of strain suggest that the decreasing values of true stress reflect the decreasing strain rate associated with the increase in specimen length. The degree of decrease in stress is masked slightly by the increasing grain size.

4) Grain growth is encouraged during deformation. Although the effect of the rate of grain growth was unresolved it is expected to be an important parameter in superplastic deformation in that the instantaneous grain size affects the strain rate sensitivity parameter m. The grain growth was shown to follow a linear logarithmic dependence with strain.

5) The apparent activation energy of the rate controlling process is approximately 10 kcal/g.atom. A model incorporating grain boundary shear and "explosive grain growth" is proposed to account for the superplastic behavior in this system. Although activation energy considerations cannot distinguish between grain boundary migration and dislocation climb it is felt that the former is the rate controlling process as it will determine the rate at which grain boundary shear can occur.

6) In regions where the deformation is slip controlled the yield stress dependence on grain size obeyed the Hall-Petch relationship: $\sigma_{0.2} = \sigma_o + Kd^{-1/2}$ where K was measured to be approximately 45,000 psi $(\text{micron})^{1/2}$ and σ_o was negligible.

6. SUGGESTIONS FOR FUTURE WORK

Several lines of investigation are suggested from the discussion of the present work. These include:

1) An investigation of superplastic deformation utilizing constant strain rate testing conditions. Since the rate sensitivity parameter is strong function of strain rate, any analysis is complicated when the strain rate is continually decreasing during testing.

2) An extensive study on how the rate of grain growth is affected by strain rate, temperature and amount of second phase present.

3) A study involving the variation of amount and nature of second phase in the alloy in an attempt to achieve a finer, more stable grain size.

APPENDIX I

Evaluation of the Strain Rate Sensitivity Parameter

The strain rate sensitivity parameter m as described by the relationship $\sigma = K\dot{\varepsilon}^m$ is the slope of the log stress-log strain rate curve, or more explicitly, $m = \partial \ln\sigma / \partial \ln \dot{\varepsilon}$. This value may be obtained graphically by measuring the slope of the σ-$\dot{\varepsilon}$ curve or by utilizing a technique described by Backofen et al (Trans. ASM 57 (1964) 980). The procedure involves making incremental changes in crosshead speed. The accompanying schematic diagram represents a change of crosshead speed from ν to ν' at a time t_1. The loads are measured at times A and B, the latter being the time at which the extrapolated curve at speed ν would reach an identical amount of strain as at speed ν' and time A. The value of m can then be calculated from:

$$m = \frac{\log {}^{P_A}/_{P_B}}{\log {}^{\nu'}/_{\nu}}$$

and is associated with the lower strain rate of $\dot{\varepsilon} = {}^{\nu}/_{\ell_B}$ where ℓ_B is the specimen length at time B.

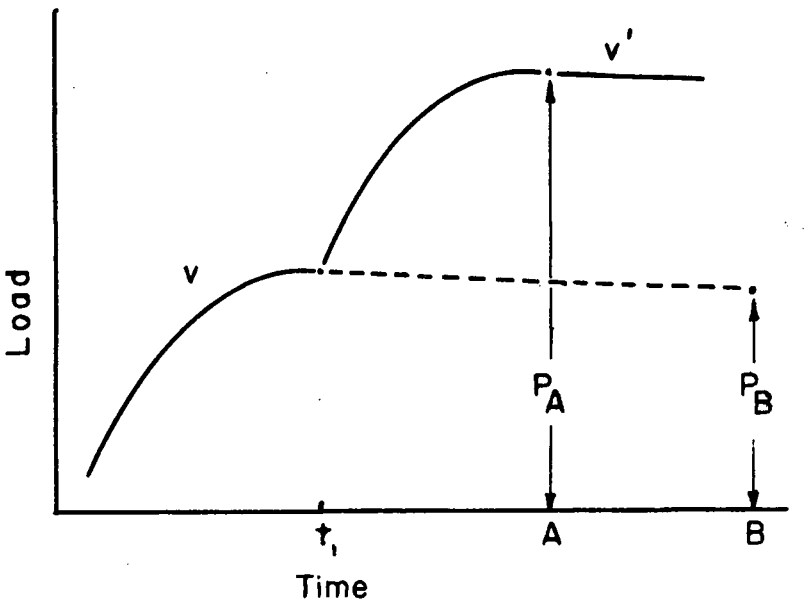

The crosshead speed was varied from 2.0×10^{-4} in./min. up to 1 in./min. in steps in which the ratio ν'/ν was either 2 or 2.5.

APPENDIX II

Various Specimens Deformed to Failure at Different Strain Rates

The extensive amounts of essentially neck-free deformation that occur in superplastic materials are worthy of presentation in pictorial form as well as graphical. Included in the following photograph are tensile specimens in the as strained condition both for the extruded casting and rolled stock. Several of the specimens shown exhibit more than one neck along the gauge length which would indicate that a neck may develop during the test but due to the local increase in strain rate, and a high value of m, the region of an incipent neck work hardens and failure does not occur at the initial cross-sectional irregularity.

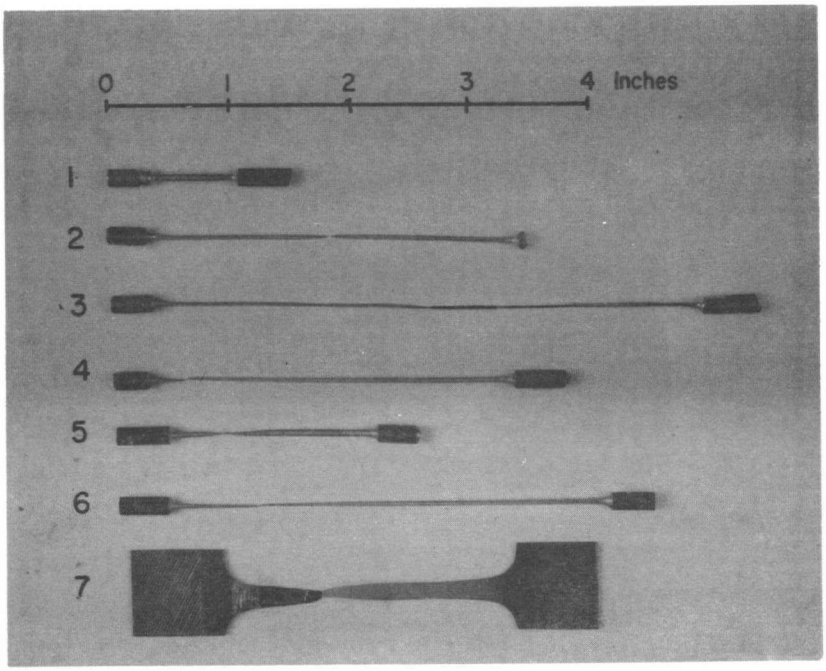

Description	Initial Strain Rate ($min.^{-1}$)	Initial m	Total Strain (%)
1. Condition A (Table I)	-	-	0
2. "	0.077	0.2	365
3. "	0.0077	0.5	590
4. "	0.0031	0.6 (maximum)	350
5. Condition B	0.0154	0.2	157
6. "	0.00154	0.6	457
7. Condition C	0.00031	0.15	216

BIBLIOGRAPHY

1) A. A. Bochvar and Z. A. Sviderskaia, Izv. Akad. Nauk., SSSR, Otdel, Tekh Nauk., 9 (1945) 821.

2) E. E. Underwood, J. Metals, 14 (1962) 914.

3) W. A. Backofen, I. R. Turner, and D. H. Avery, ASM Trans. Quart., 57 (1964) 980.

4) D. H. Avery and W. A. Backofen, ASM Trans. Quart., 58 (1965) 551.

5) D. Lee and W. A. Backofen, Trans. AIME, 239 (1967) 1034.

6) T. H. Alden, Acta. Met., 15 (1967) 469.

7) H. E. Cline and T. H. Alden, Trans. AIME., 239 (1967) 710.

8) D. L. Holt and W. A. Backofen, ASM Trans. Quart., 59 (1966) 755.

9) T. H. Alden and H. W. Schadler, Trans. AIME., 242 (1968) 825.

10) P. J. Martin and W. A. Backofen, ASM Trans. Quart., 60 (1967) 352.

11) S. W. Zehr and W. A. Backofen, ASM Trans. Quart., 61 (1968) 300.

12) D. L. Holt, Trans. AIME, 242 (1968) 25.

13) E. W. Hart, Acta. Met., 15 (1967) 1545.

14) H. W. Hayden, R. C. Gibson, H. F. Merrick and J. H. Brophy, ASM Trans. Quart., 60 (1967) 3.

15) D. Oelochlagel and V. Weiss, ASM Trans. Quart., 59 (1966) 143.

16) D. L. Holt, Trans. AIME, 242 (1968) 740.

17) C. M. Packer and O. D. Sherby, ASM Trans. Quart., 60 (1967) 21.

18) R. Kossowsky and J. H. Bechtold, Trans. AIME, 242 (1968) 716.

19) T. H. Alden, Trans. AIME, 236 (1966) 1633.

20) T. H. Alden, to be published, ASM Trans. Quart.

21) D. Tromans and J. A. Lund, ASM Trans. Quart., 59 (1966) 672.

22) R. C. Gifkins, J. Inst. Metals, 95 (1967) 373.

23) C. E. Pearson, J. Inst. Metals, 54 (1934) 111.

24) W. Schulze and F. Sauerwald, Z. Metallkunde, 53 (1962) 660.

25) T. H. Alden, Discussion, ASM Trans. Quart., 60 (1967), 274.

26) R. B. Jones and R. H. Johnson, Discussion, ASM Trans. Quart., 59 (1966) 356.

27) S. Floreen, Scripta Met., 1 (1967) 19.

28a) N. F. Mott, Phil. Mag. 44 (1953) 742.

b) N. F. Mott, Proc. Phys. Soc., B64 (1951) 729.

29a) J. Friedel, "Les Dislocations", Gauthier-Villars, Paris (1956) 176-179, 198-201.

b) J. Friedel, "Dislocations", Addision-Wesley (1964), Reading, Mass., First English Edition pp. 299 and 315.

30) C. J. Smithells, "Metals Reference Book", vol. 2, Butterworth's London (1962).